

GEOLOGY FOR SOCIETY

SINCE 1858



**GEOLOGICAL
SURVEY OF
NORWAY**

· NGU ·



Report no.: 2017.021		ISSN: 0800-3416 (print) ISSN: 2387-3515 (online)		Grading: Open	
Title: Geophysical and geological investigations of Hesten, Vardfjellet and Grunnvåg graphite occurrences, Senja, Northern Norway.					
Authors: J.S. Rønning, H. Gautneb, I.H.C. Henderson, B.E. Larsen, J. Knezevic, J. Gellein, & F. Ofstad.			Client: Troms fylkeskommune/NGU		
County: Troms			Commune: Lenvik		
Map-sheet name (M=1:250.000) Tromsø			Map-sheet no. and -name (M=1:50.000) 1433-4 Melfjordbotn		
Deposit name and grid-reference: WGS 84 UTM 33 Hesten: 609270 – 7702780, Vardfjellet,: 607420 – 7705050, Grunnvåg: 617700 - 7702320			Number of pages: 72 Map enclosures:		Price (NOK): 200,-
Fieldwork carried out: August 2016		Date of report: 18.05.2017		Project no.: 371100	Person responsible: <i>Marco Brönnert</i>
<p>Summary: As a part of the MINN project (Minerals in Northern Norway) a helicopter-borne geophysical survey were performed at Senja in 2012 – 2014. Electromagnetic data from this survey showed up anomalies that could be caused by large graphite mineralisations. Geophysical and geological follow-up work was carried out at three locations in 2016, Hesten, Vardfjellet and Grunnvåg, with additional funds from the Troms County administration. A new showing at Grunnvåg was discovered in a short geological visit.</p> <p>At Hesten, possible graphite mineralisation is mapped in a length of ca. 2 km with a width varying from ca. 100 m to ca. 400 m. Most likely there are several graphite zones. The individual thickness is measured to be 3 – 4 m at two locations, and the dip is observed to be ca. 70° to the west. Charge Potential measurements indicate that the graphite bodies are electrically connected and the size (length and depth extend) of the individual zones is not possible to map. Graphite appears as 50 to 2000 micron flake minerals. The average graphite carbon content (Cg) of 21 samples is 5.5 % with a maximum value of 12.8 %. Total sulphur content is < 1 %. Previous geological mapping shows that the graphite schist on the surface consists of several apparently isolated lenses that are isoclinally folded and refolded and several deformations have influenced on the graphite structures.</p> <p>At Vardfjellet, the graphite mineralisations are more exposed and graphite can be found in a total length of 2 km and with a width that varies from ca. 100 m to ca. 480 m. Most likely there are several steeply dipping graphite zones. The thickness observed to be 7 m at one location, and measured to be 3 – 5 m at two others. Measurements indicate that the graphite bodies are electrically connected and the size of the individual zones is not possible to map. Graphite appears as 50 to 2000 micron flake minerals. The average graphite carbon content (Cg) of 37 samples is 9.2 % with a maximum value of 40.3 %. Total sulphur content is < 1.3 %. Previous geological mapping shows that the graphite schist on the surface also here consists of several apparently isolated lenses that are isoclinally folded and refolded and several deformations have influenced on the graphite structures.</p> <p>At Grunnvåg, a ca. 1.5 km and ca. 100 m wide helicopter-borne apparent resistivity anomaly appeared. A short geological inspection discovered graphite that are dissected and intruded by mafic and granitic rock. The average graphitic carbon content of 5 samples where 8.9 % with a maximum value of 14.8 %. The sulphur content is higher at this location, up to 12.5 %.</p> <p>The mineralogy of the graphite schist on Senja is essentially the same as in the Vesterålen area, where successful beneficiation tests were performed. Here it was possible to get a final graphite concentrate with more than 95 % graphite carbon with good recovery. The same kind of results is expected for the graphite reported here.</p>					
Keywords: Graphite		Geology		Geophysics	
Electromagnetic		Electrical		3D Photogrammetry	
Mapping		Analytical methods		Scientific report	

Executive summary

Purposes:

- To investigate previously known and possible new graphite mineralisations associated with airborne geophysical anomalies.
- To investigate with ground geophysical methods (CP/SP and ERT/IP), the mineralized areas.
- To sample outcropping graphite bearing rocks as representative as possible.
- To perform 3D structural modelling of the mineralisations.

Two main areas were investigated: The Hesten and Vardfjellet mountains and some observations from one additional locality (Grunnvåg).

Results:

The area is a high-grade metamorphic terrain, which is favourable for formation of flake graphite deposits.

The mineralised areas have approximately dimensions as follows:

Hesten: 2 km x 0.3 km

Vardfjellet: 2 km x 0.5 km

Grunnvåg: 1.5 km x 0.1 km

At both Hesten and Vardfjellet, the graphite occurs in several mineralised zones of flake graphite that in the field are strongly polyphase folded. Individual graphite lenses can be followed outcropping continuously up to about 100 meters. Geophysical measurements indicate the individual lenses to be electrically connected restricting the possibility to map the individual size (length and depth extend) of the graphite lenses. The graphite bearing units are mostly steeply dipping (70°-90°). The complex deformation makes it difficult to get an exact overview of the total and individual thicknesses of the different graphite lenses. Drilling would be necessary to get a good understanding of grades and tonnages.

The table below shows the analytical results % Cg (total carbon) from the different localities:

Locality	No of samples	Average (%Cg)	Max (% Cg)	Min (%Cg)	Stdvp
Vardfjellet	37	9.2	40.3	1.1	7.5
Hesten	21	5.8	12.8	1.7	3.0
Grunnvåg	5	8.9	14.8	6.7	3.4
Total	63	8.0	40.3	1.1	6.2

There is a large and mostly unsystematic spatial variation in the levels of graphitic carbon.

The mineralogy of the graphite bearing rock is similar to what is in production at Skaland and with all probability the rock can be beneficiated with similar good results.

Recommendations

We regard Hesten and Vardfjellet to be investigated as detailed as possible, with surface methods only, and to the degree that is relevant for NGU. It is recommended that drilling is done on each locality to get a better understanding of thickness and graphite grade of individual graphite bearing zones and to make a preliminary tonnage estimate. 5 to 7 drill holes of 150 to 200 meters length would give a first tonnage estimate.

The neighbouring Bukken (Bukkemoen) and Grunnvåg should also be investigated in the same manner as the present study of Vardfjellet and Hesten.

Sammendrag på norsk.

Som en del av prosjektet Mineralressurser i Nord-Norge (MINN) ble det i 2012 – 2014 foretatt geofysiske målinger fra helikopter på den nordlige delen av Senja hvor det er et stort potensiale for økonomiske grafittforekomster. Disse målingene viste flere markerte elektromagnetiske anomalier, delvis knyttet til kjente forekomster og delvis på mulige nye hittil ukjente forekomster. For å øke kunnskapen om de enkelte mineraliseringene foreslo NGU i 2016 et oppfølgingsprosjekt som ble gjennomført med støtte fra Troms fylkeskommune. Flere forekomster var aktuelle hvorav mineraliseringene på Hesten og på Vardfjellet ble prioritert for undersøkelser i 2016. Bukken, eller Bukkemoen, ble prioritert for 2017 sammen med området kalt Grunnvåg.

Ved fjellet **Hesten**, sentralt på Senja, er det påvist grafitt i en lengde på ca. 2 km og med en bredde på ca. 100 til ca. 400 m. Det mineraliserte området består av flere soner og individuell tykkelse er målt til 3-4 meter ved to plasser. Geofysiske målinger viser at de enkelte linsene er i elektrisk kontakt med hverandre og en vurdering av de individuelle størrelsene (lengde og dyptgående) er ikke mulig å tolke på grunnlag av geofysikk. Grafitten opptrer som "flake" og kornstørrelse på fra 50 til 2000 mikron. Gjennomsnittlig innhold av grafittisk karbon (Cg) på 21 fastfjellsprøver fra området er på 5,5 % med en maksimumsverdi på 12,8 %. Svovelinnholdet er mindre enn 1 %. NGU anbefaler videre undersøkelser i form av detaljerte elektromagnetiske målinger på bakken og oppfølgende boringer.

Ved fjellet **Vardfjellet**, ca. 2,5 km nord for Hesten er det også påvist grafitt i en lengde på ca. 2 km men med en bredde på ca. 100 til ca. 480 m. Det mineraliserte området består av flere soner og individuell tykkelse observert til 7 m og er målt til 3-4 meter ved to plasser. Geofysiske målinger viser at de enkelte linsene er i elektrisk kontakt med hverandre og en vurdering av de individuelle størrelsene (lengde og dyptgående) er ikke mulig å tolke på grunnlag av geofysikk. Grafitten opptrer som "flake" og kornstørrelse på fra 50 til 2000 mikron. Gjennomsnittlig innhold av grafittisk karbon (Cg) på 37 fastfjellsprøver fra området er på 9,2 % med en maksimumsverdi på 40,3 %. Svovelinnholdet på de samme prøvene er mindre enn 1,3 %. NGU anbefaler videre undersøkelser i form av detaljerte elektromagnetiske målinger på bakken og oppfølgende boringer.

Ved **Grunnvåg**, i botn av Lysfjorden, er det påvist en elektromagnetisk anomali fra helikoptermålingen som er 1,5 km lang og opp til ca. 100 m bred. Ved en geologisk befaring her ble det påvist og prøvetatt grafitt. Gjennomsnittlig innhold av grafittisk karbon (Cg) på 5 fastfjellsprøver fra området er på 8,9 % med en maksimumsverdi på 14,8 %. Svovelinnholdet er høyere her, opptil 12,5 %.

Felles for disse tre mineraliseringene er at grafitten er av meget god kvalitet og ligner grafitten det drives på ved Skaland grafittverk og den som er oppredningstestet med godt resultat fra Vesterålen. NGU mener den undersøkte grafitten fra Senja lett kan oppredes til konsentrat med høy konsentrasjon og med god gjenvinning. Ved **Hesten** og **Vardfjellet** anbefales detaljerte elektromagnetiske målinger på bakken forut for diamantboring. Dette må finansieres og gjennomføres med finansiering fra et prospekteringselskap. Ved **Grunnvåg** og ved **Bukken (Bukkemoen)** anbefales undersøkelser av samme type som de som er utført ved Hesten og på Vardfjellet.

Contents

1. INTRODUCTION.....	13
1.1 Physiography and landownership	13
2. GEOLOGICAL SETTING.....	16
3. HISTORICAL BACKGROUND AND PREVIOUS INVESTIGATIONS.....	17
3.1 Structural geology of the graphite mineralisation and associated rocks	17
3.2 Geophysical investigations.....	18
4. GEOPHYSICAL, GEOLOGICAL AND PHOTOGRAMMETRY METHODS	18
4.1 Geophysical methods.....	18
4.1.1 Helicopter-borne Electromagnetic Measurements	18
4.1.2 Charged Potential and Self Potential methods	20
4.1.3 2D resistivity and Induced Polarization (IP).....	22
4.2 Geological methods.....	24
4.3 Aerial photogrammetry.....	24
4.3.1 Equipment.....	24
4.3.2 Uncertainty in the modelling.....	29
5. SELECTION OF FOLLOW-UP OBJECTS.....	30
6. RESULTS OF GROUND GEOPHYSICAL INVESTIGATIONS	33
6.1 Geophysical results, Hesten	33
6.1.1 CP measurements at Hesten.....	34
6.1.2 SP measurements at Hesten.....	36
6.1.3 2D Resistivity/IP at Hesten.....	39
6.2 Geophysical results, Vardfjellet	41
6.2.1 SP measurements at Vardfjellet.....	42
6.2.2 2D Resistivity/IP at Vardfjellet.....	45
7. RESULTS OF GEOLOGICAL INVESTIGATIONS	46
7.1 Geological investigations at Hesten.....	46
7.2 Geological investigations at Vardfjellet.....	47
7.3 Geological investigations at Grunnvåg.....	49
7.4 Petrography of graphite bearing rocks	51
7.5 Modal content of graphite	53
7.6 Summary of sulfide and carbon analysis	53
8. 3D PHOTOGRAMMETRY AND GEOLOGICAL MODELLING	55
8.1 3D drone photogrammetry modelling at Hesten	55
8.2 3D drone photogrammetry modelling at Vardfjellet.....	57
9. SUMMARY AND CONCLUSIONS.....	60
9.1 Summary and conclusions, Hesten	60
9.2 Summary and conclusions, Vardfjellet.	61
9.3 Summary and conclusions, Grunnvåg	62
9.4 Benification test.....	62
10. REFERENCES.....	63

FIGURES

Figure 1.1: Geology of Norway and graphite provinces of Norway.	14
Figure 1.2: Landscape view of the investigated area seen from the top of Vardfjellet (639 m.a.s.l) towards Hesten (496 m.a.s.l), with lake Hestvannet just to the left, lake Lysvatn in the background.	14
Figure 1.3: The occurrences (centerpoint) plotted on the cadastral map of the area.....	15
Figure 2.1: The geology of the west Troms basement complex and location of the investigated area (modified from Myhre et al. 2013).	16
Figure 4.1: Equipment used in the helicopter-borne geophysical survey in Vesterålen.	19
Figure 4.2: Conceptual illustration of the CP- method. The current electrode (C_1) is connected to the ore body and the remote electrode (C_2) is placed far outside the survey area. The color indicates the strength of the charged potential above an ore-body. The dashed line shows the survey path along which the entire body will eventually be covered..	20
Figure 4.3: Establishing CP ore grounding point and data acquisition in combined CP and SP measurements.	21
Figure 4.4: Diagram of measuring procedure illustrating the setup of the Lund System and the roll-along method for performing as many measurements as required. From (ABEM, 2012).....	22
Figure 4.5: Summary of the workflow process developed at NGU to construct 3D topographic-geological models from aerial photos.....	25
Figure 4.6: The drone used to acquire GPS-rectified images from the air- the DJI Phantom 4.	25
Figure 4.7: The control unit for the DJI Phantom 4 drone with accompanying Ipad. This is used to remotely control the drone with the <i>Litchi</i> application.	25
Figure 4.8: The principal of construction of a 3D elevation model from 2D static images taken from a drone.....	26
Figure 4.9: Automatic flight-plan construction in ArcGIS. This produces a .csv file with XYZ points that can be uploaded to the drone.....	27
Figure 4.10: Image from the Litchi application which controls the drone automatically in the air.	27
Figure 4.11: Construction of the elevation model with the software <i>Agisoft Photoscan Professional</i> from Vardfjellet. A: Images uploaded to the software. The images are shown in blue. This 'light' point cloud has over 40 000 points. B: dense point cloud. The calculated points are so dense that they begin to look like a surface. The software program has calculated over 15 million points. C: elevation model created from the dense point cloud. Here there are over 1 million surfaces. D: Finished elevation model with images.	28
Figure 4.12: Image of finished elevation model for Hesten with orthophotos in 3D MOVE ready for the input of geological data.....	29
Figure 5.1: Apparent resistivity (7001 Hz) and graphite mineralisations on Senja. T= Trælen, S= Skaland, G= Geitskaret, K= Krokeldal, SK= Skarsvåg, VF= Vardfjellet, H=Hesten. B=Bukken, BØ= Bukken East and GR= Grunnvåg.	30
Figure 5.2: Apparent resistivity anomalies proposed for follow-up investigations on Senja, Vardfjellet, Hesten, Bukken and Grunnvåg.	31
Figure 6.1: Apparent resistivity calculated from 7001 Hz coaxial coils at Hesten. Location of CP grounding point and 2D resistivity/IP profile is given as green star and blue line respectively.	33
Figure 6.2: Results of CP measurements at Hesten with SP anomalies superimposed. The measured CP measuring points are the same as SP points.	35
Figure 6.3: Results of SP measurements at Hesten on top of apparent resistivity from helicopter-borne EM measurements (7001 Hz, from Rodionov et al. 2014).	37
Figure 6.4: SP anomalies at Hesten superimposed at geological map modified from Henderson & Kendrick (2003). Cross section is not to scale.....	38
Figure 6.5: 2D resistivity (top) and IP (bottom) results along profile 1 at Hesten. Known graphite outcrops are indicated with red arrows, possible (interpreted) graphite zones with black arrow.....	39

Figure 6.6: Apparent resistivity calculated from 7001 Hz coaxial coils at Vardfjellet. Location of CP grounding point and 2D resistivity/IP profile is given as green star and blue line.....	41
Figure 6.7: Results of SP measurements at Vardfjellet superimposed at apparent resistivity (7001 Hz, from Rodionov et al. 2014).	43
Figure 6.8: SP anomalies at Vardfjellet superimposed at geological map modified from Henderson & Kendrick (2003). Cross section is not to scale.....	44
Figure 6.9: 2D resistivity (top) and IP (bottom) results along profile 1 at Vardfjellet. Known graphite outcrops is indicated with red arrows, possible (interpreted) graphite zones with black arrow.....	45
Figure 7.1: Graphite sampling points and analyzed graphitic carbon content at Hesten. The background is apparent resistivity calculated from frequency EM 7001 Hz (See Rodionov et al., 2014 for geophysical details).	47
Figure 7.2: The southern side of Vardfjellet with some of the graphite lenses and sample point and analyses indicated. Total width of the graphite schist is ca. 7 m.....	48
Figure 7.3: Rock face (about 150 m long) on the western side of Vardfjellet comprising a mixture of graphite schist and sulfide bearing quartz and feldspar rich rock. (sample points and analyses are indicated).....	48
Figure 7.4: Graphite sampling points and analysed graphitic carbon content at Vardfjellet. The background is apparent resistivity calculated from frequency EM 7001 Hz (See Rodionov et al., 2013 for geophysical details).	49
Figure 7.5: Location of sample points at Lysbotn next to Grunnvåg plotted on apparent resistivity (7001 Hz, After Rodionov et al. 2014).	50
Figure 7.6: Outcrops of graphite schist cut by mafic and acid igneous rocks at the innermost part of Lysbotn (graphite bearing zones are indicated).	50
Figure 7.7: Thin section photo of graphite schist from Hesten sample Hg39-16.....	52
Figure 7.8: Thin section photo of graphite schist from Vardfjellet sample Hg45-16.....	52
Figure 8.1: View of the Hesten deposit seen from the south east, showing the elevation model with the orthophotos draped over the elevation model. The white arrow shows the trend of a series of outcrops which is observed as a grey/brown colour in the model and is the linearly outcropping graphite.....	55
Figure 8.2: View of the Hesten deposit seen from the south east, showing the elevation model with the orthophotos draped over the elevation model. The elevation model is made transparent such that the geology is visible. The enveloping meta-supracrustals are seen in green and the graphite layers in blue. The northern margin of the deposit (right) is truncated by an east west fault.....	56
Figure 8.3: View of the Hesten deposit seen from the east, showing the EM anomaly map over the elevation model. The elevation model is made transparent such that the geology is visible. The enveloping amphibolitic schists are green and the graphite layers are blue. The EM anomaly coincides with the general exposure of the folded graphite layers.....	56
Figure 8.4: View of the Vardfjellet deposit seen from the south east, showing the elevation model with the orthophotos draped over the elevation model.	57
Figure 8.5: View of the Vardfjellet deposit seen from the south east, showing the elevation model with the orthophotos draped over the elevation model. The elevation model is made transparent such that the geology is visible.	58
Figure 8.6: The northern part of the Vardfjellet deposit showing the complexly folded graphite (blue) and the enveloping greenstone rocks (green). In this part of the deposit, the generally N-S F2 fold axes of the greenstones are deformed around open F3 fold hinges such that the F2 fold hinges are E-W. The F3 fold hinge is complexly dissected by F3 faults and shear zones (red).	59
Figure 8.7: View of the Vardfjellet deposit seen from the east, showing the EM anomaly map over the elevation model. The elevation model is made transparent such that the geology is visible- The enveloping amphibolitic schists are green and the graphite layers are blue. The EM anomaly coincides with the general exposure of the complexly folded graphite layers. ...	59

TABLES

Table 4.1: Instrumentations used in helicopter-borne geophysical survey.	18
Table 4.2: Configuration and frequencies of the Hummingbird EM recorder.	19
Table 4.3: 2D resistivity/IP. Number of measured, removed and remaining data points for inversion.	23
Table 6.1: Coordinates (WGS 84, UTM Zone 33), applied current and no. of measured points used for CP measurements at Hesten. R1 is the remote electrode.	34
Table 6.2: Coordinates (WGS 84, UTM Zone 33), applied current and no. of measured points used for CP measurements at Vardfjellet. R2 is the remote electrode.	42
Table 7.1: Weight % of total sulphur (TS) and graphitic carbon (Cg) in samples from Grunnvåg.	51
Table 7.2: Modal % of graphite and weight percent of graphitic carbon (Cg) in some selected samples from Hesten, Vardfjellet, Bukkemoen and Grunnvåg.	53
Table 7.3: Summary of graphitic carbon content in samples from Hesten, Vardfjellet and Grunnvåg.	53

APPENDIX

Appendix 1 Analyses of sulphur and carbon from Vardfjellet, Hesten and Grunnvåg.	65
Appendix 2: Selected thin section images.	68
Appendix 3: Geological map over Vardfjellet and Hesten from Henderson & Kendrick ...	72

1. INTRODUCTION

Norway has been a major producer of graphite for more than 100 years and in many places in the country the geology favours the formation of flake graphite deposits. Graphite is a common mineral in Norwegian rocks, however it is rare to find it enriched in economically interesting amounts. There are more than 70 registered graphite occurrences in Norway. They are located in four graphite provinces (Figure 1.1). In all of these provinces there has been historic graphite mining. Today only one deposit, the Skaland graphite mine on the island of Senja, is in operation, producing approximately 9000 tons of concentrate per year. The island of Senja has a number of other graphite occurrences.

In this report we will present the data and results from recent graphite exploration on two of the largest graphite occurrences on Senja. We will also give a brief review of the earlier work in the area. In every chapter we will limit our descriptions to what is regarded relevant for the graphite mineralisation. More academic type of studies of the general geology and metamorphic petrology are reported by others elsewhere.

During the work the following people have contributed with their different fields of expertise:

- Håvard Gautneb, graphite geology, analysis and petrography, responsible field geologist
- Jomar Gellein, Ground geophysics
- Iain Henderson, Structural geology, aerial photography and 3D modelling.
- Janja Knezevic, graphite geology, ground geophysics and sample preparation, GIS
- Janusz Koziel, instrumentation
- Bjørn Eskil Larsen, responsible field geophysicist, GIS
- Frode Ofstad, airborne and ground geophysics, electronics
- Jan Steinar Rønning, responsible geophysicist, reporting, report editing and project leader.

The investigations are financially supported by Troms County Administration; the investigations are planned for two years. This first year, the investigations were concentrated at Hesten and Vardfjellet. For the second year (2017), investigations at Bukkemoen and Grunnvåg are planned.

1.1 Physiography and landownership

Mount Hesten (The Horse) and Mount Vardfjellet (Cairn Mountain) are situated 2-4 km north of the Lysvann power station in the east-central part of the Senja island (Figure 1.3). The areas are most practically accessed with the use of four wheel ATV vehicles (a permit for use of off-road vehicles is needed from the local municipality, Lenvik). From Lysvann to the top of the Vardfjellet mountain is approximately a one hour drive with ATV. From Lysvann to the city of Finnsnes the drive is about 40 minutes on an allweather road. The nearest quay is located at Gibostad about 20 minutes on an all weather road from Lysbotn. Hesten and Vardfjellet mountains are totally uninhabited. The land is public and administrated by the State owned

enterprise Statskog (www.statskog.no). The cadastral map of the area can be seen in (Figure 1.3) or www.seiendom.no . During normal annual snow conditions all parts of the investigated area can be accessed from early July to the end of October. Snow can be expected at the mountain tops from mid-October. A landscape view of the area is shown in Figure 1.2. Prospectors interested in this area should check the web sites of the Norwegian Directorate of mining (www.dirmin.no) for Norwegian mining regulations.

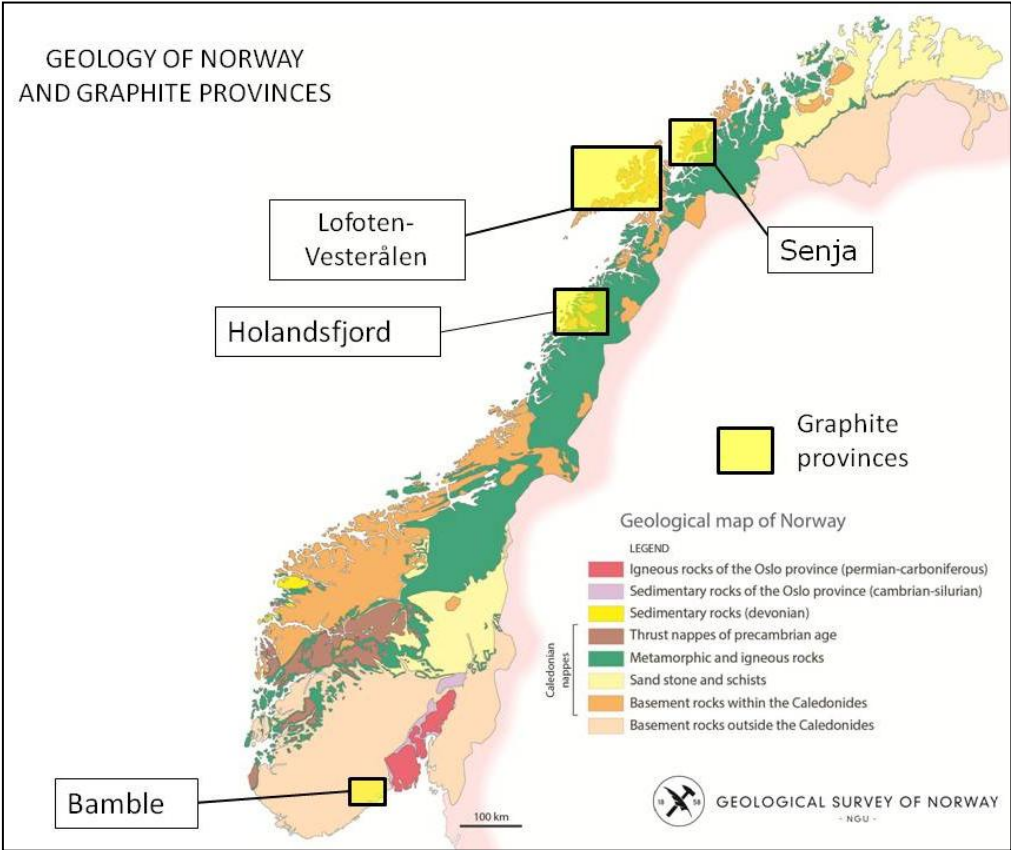


Figure 1.1: Geology of Norway and graphite provinces of Norway.

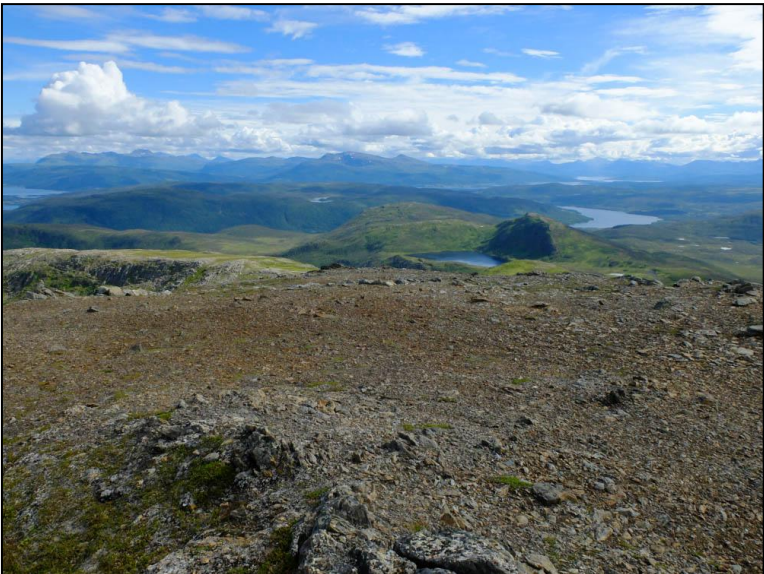


Figure 1.2: Landscape view of the investigated area seen from the top of Vardfjellet (639 m.a.s.l) towards Hesten (496 m.a.s.l), with lake Hestvannet just to the left, lake Lysvatn in the background.



Figure 1.3: The occurrences (centerpoint, red dots) plotted on the cadastral map of the area.

2. GEOLOGICAL SETTING

The investigated area is part of the West Troms Basement complex that constitutes the coastal area of Troms (Figure 2.1). This region comprises Archean gneisses of variable origin, Archean and Palaeoproterozoic greenstone belts and Svecofennian bimodal intrusions with an age of approximately 1.8 Ga. The geology of the West Troms Basement complex is described by Myhre et al. (2013 and references there in). According to Myhre et al. (2013) the West Troms Basement complex comprises three stages of Archean magmatism and one superimposed Neoproterozoic high grade metamorphic event. The three magmatic events are dated to 2.92-2.8 Ga, 2.75-2.70 Ga (main phase) and 2.70-2.67 Ga respectively. The Neoproterozoic metamorphic event involved stromatic migmatite formation and is dated to 2.70-2.67 Ga. These migmatites locally contain remnants of supracrustal rocks of volcanic and sedimentary origin. Their age is uncertain. The supracrustal rocks are today seen as marbles, hornblende biotite gneisses, graphite schist, quartzites and garnet mica schist.

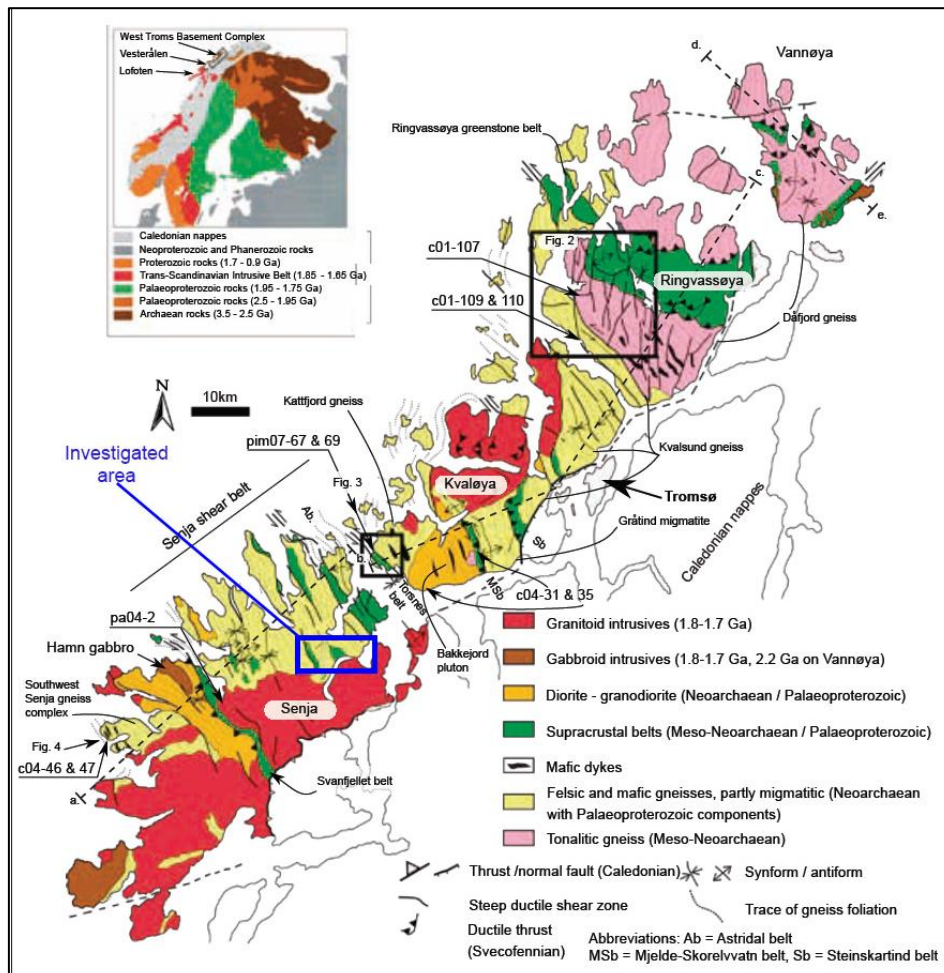


Figure 2.1: The geology of the west Troms basement complex and location of the investigated area (modified from Myhre et al. 2013).

During the Svecofennian orogeny (1.8-1.7 Ga) the West Troms Basement complex was reworked, metamorphosed and intruded by mafic to felsic intrusions. A more specific description of the geology and structural controls of the graphite-bearing rocks are given in chapter 3.

3. HISTORICAL BACKGROUND AND PREVIOUS INVESTIGATIONS

The graphite deposits of Senja were among the first that were described by geologist in Norway. Keilhau (1844) described the graphite occurrences at Trælen (Lyktgangen). This deposit had probably already been known for some time. The Skaland deposit was discovered around 1870. Mining started here in 1917. Modern mining started in 1932 and continues to the present day. In 2006 the reserves at Skaland were exhausted, and the mine moved to Trælen where operations today produce approximately 9000 tons of graphite concentrate annually. Apart from unpublished (and confidential) reports, little is published about the graphite mineralisation on Senja.

A bedrock geological map in scale 1:50.000 is published by Zwaan & Fareth (2005).

3.1 Structural geology of the graphite mineralisation and associated rocks

Heldal & Lund (1987) first studied in detail the various graphite deposits on the island of Senja. The most comprehensive general study of the structural geology of the graphite mineralisation is that of Henderson & Kendrick (2003) which presents geological mapping and structural analysis of many graphite occurrences on Senja. This study includes detailed structural analysis of 6 of these graphite deposits. Detailed 1:5.000 structural mapping was undertaken on 4 of these deposits along with sample collection for graphite content analysis. Regional observations were also made to supplement the structural knowledge gained from the deposits and to put their geometries in a regional context.

Henderson & Kendrick (2003) characterized the complex structural episodes to have both created and modified the graphite deposits and found that the graphite is intimately associated with the development of F_2 folds, as graphite is best developed geographically in association with north-south striking F_2 fold hinges. However, the F_2 fold hinges are deformed by D_3 deformation on approximately E-W axes. This created complex interference geometries. The graphite is most geographically extensive where F_3 structures intersect graphite-bearing F_2 structures. The extent of graphite outcrop is also strongly affected by the presence of both F_2 and F_3 shear zone structures which locally (F_2) or regionally (F_3) 'shear-out' the graphite outcrops, thereby limiting the extent of the graphite deposits. Therefore a good knowledge of the combination of the D_2 and D_3 structures will allow for a better understanding of the geometry of the graphite deposits.

At the Trælen and Finnkona deposits an additional deformation episode was identified (D_4). In many of the deposits both the F_2 and F_3 folding is highly non-cylindrical, demonstrating that using small-fold geometries to determine the large scale deposit geometry is highly problematic. It was summarized by Henderson & Kendrick (2003) that great care should be taken in further prospecting for graphite deposits on Senja.

3.2 Geophysical investigations

Detailed geophysical investigations have earlier been performed on the following graphite occurrences:

- Krokeldalen, (Dalsegg 1985)
- Geitskaret, (Dalsegg 1985)
- Skaland, (Dalsegg 1986, Rønning et al.2012)
- Bukkemoen (Lauritzen 1988).

In the period 2012 to 2014, northern Senja was covered by helicopter-borne geophysics, including magnetic, electromagnetic and radiometric data (Rodionov et al. 2014). A more comprehensive description is given in chapter 4.

4. GEOPHYSICAL, GEOLOGICAL AND PHOTOGRAMMETRY METHODS

The resolution of helicopter-borne electromagnetic measurements is low and detailed ground measurements are necessary to achieve a good knowledge of the graphite deposits. Here we describe the methods used in the graphite investigations in 2016.

4.1 Geophysical methods

In the graphite investigations on Senja, we have used the following geophysical methods: Helicopter-borne electromagnetic (HEM), Charged Potential (CP), Self Potential (SP), 2D Resistivity (also called ERT) and Induced Polarisation (IP).

4.1.1 Helicopter-borne Electromagnetic Measurements

A new helicopter-borne geophysical survey was performed in 2012, 2013 and 2014, with a total of 5620 line km covering 1124 km² in the northern part of Senja. The full technical description, including details of processing of the data collected was reported by Rodionov et al. (2014). The survey included the instrumentation listed in Table. 4.1

Table 4.1: Instrumentations used in helicopter-borne geophysical survey.

Instrument	Producer/Model	Accuracy	Sampling Frequency/Interval
Magnetometer	Scintrex Cs-2	0,002 nT	5 Hz
Base magnetometer	GEM GSM-19	0.1 nT	3 sec
Electromagnetic	Geotech Hummingbird	1 – 2 ppm	10 Hz
Gamma spectrometer	Radiation Solutions RSX-5	1024 ch's, 16 liters down, 4 liters up	1 Hz
Radar altimeter	Bendix/King KRA 405B	± 3 % 0 – 500 feet ± 5 % 500 –2500 feet	1 Hz
Pressure/temperature	Honeywell PPT	± 0,03 % FS	1 Hz
Navigation	Topcon GPS-receiver	± 5 meter	1 Hz
Acquisition system	NGU in house software		

The ElectroMagnetic (EM) instrumentation, Geotech Hummingbird (Geotech, 1997), is able to map variations in electric conductivity in the ground and is the most useful method in graphite exploration. Details about frequencies, coil orientations and coil separation are shown in Table 4.2.

Table 4.2: Configuration and frequencies of the Hummingbird EM recorder.

Coils:	Frequency	Orientation	Coil separation
A	7001 Hz	Coaxial	6.20 m
B	6600 Hz	Coplanar	6.20 m
C	980 Hz	Coaxial	6.025 m
D	880 Hz	Coplanar	6.025 m
E	34000 Hz	Coplanar	4.87 m



Figure 4.1: Equipment used in the helicopter-borne geophysical survey in Vesterålen.

The apparent resistivity for each frequency was calculated based on "In phase" and "Out of phase" components of the EM data, using a half-space model of the earth (HEM-module, (Geosoft, 1997)). Data can also be presented as profile maps, on which "In Phase" and "Out of phase" components for each frequency are plotted along the flight path.

Inverted resistivity sections can be produced based on the measured "In phase" and "Out of phase" components for each frequency. Available software is EM1DFM (Electromagnetic 1D Frequency Measurements, UBC (2000)) and AarhusInv (formerly called em1Dinv, AarhusInv (2013)). These inversion codes create 2D images based on in principle 1D inversion and with vertical conducting structures, misleading images may be constructed. For this reason, inversions of EM data from Senja were performed but are not presented here. NGU are considering 2D or 3D inversion of EM data from Senja.

The main result from this geophysical survey was a large extension of the area with potential for new graphite mineralisations, and a better definition of the areal extent of known occurrences. This was the basis for defining new graphite targets to be followed up by ground investigations. Most of the occurrences described in this report were previously known, but the mineralised area is larger than previously known.

Several new objects are derived from the interpretation of the new airborne geophysical data.

All of the data from the helicopter survey can be downloaded from www.ngu.no as jpg-maps or geo-referenced data sets (geotiff-files).

4.1.2 Charged Potential and Self Potential methods

Charged Potential (CP) measurements are acquired by connecting a current electrode directly to the conductive body and locating the other remote electrode at a considerable distance to ensure that its effect is virtually non-existent in the survey area. The current can be injected through a surface outcrop or a borehole if no outcrops are available. The potential between two non-polarizable electrodes is then measured on the surface around the conductive body in a sequence of connected measurement-points. As long as the electric conductivity of the mineralisation is more than 1000 times higher than that in the surrounding host rock, the electrical potential will, in practice, stay constant above the mineralisation, and then drop down when the measurements are outside the ore-body (Figure 4.2). By measuring the potential around a known graphite ore-body, the body's length, dip and size can be mapped. In addition, an outline of unknown ore-bodies can be mapped.

A practical way of interpreting depth extend of nearly vertical electric conductive bodies from CP data is presented by Kihle & Eidsvig (1978).

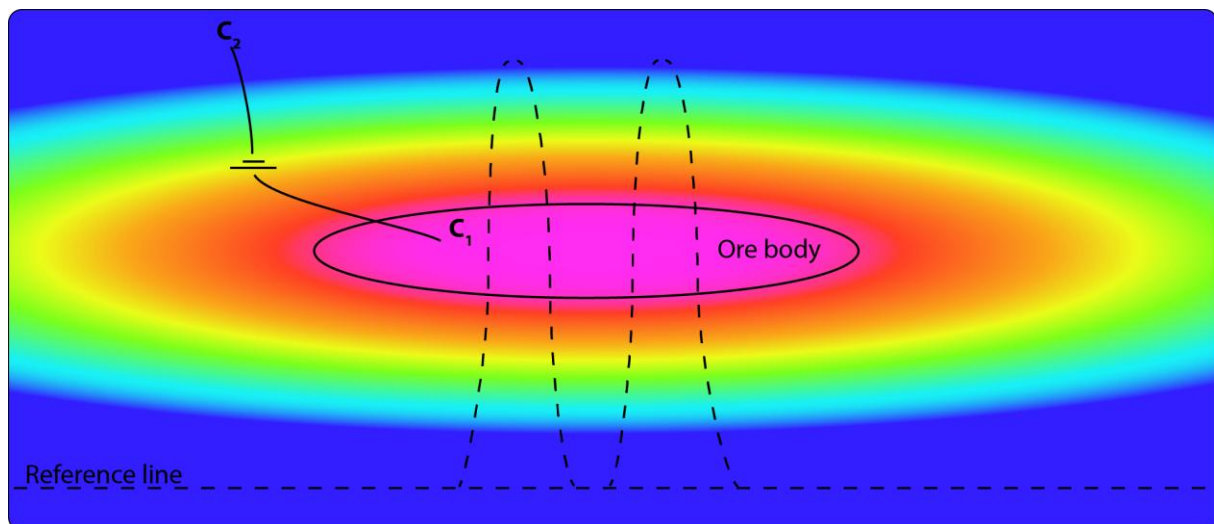


Figure 4.2: Conceptual illustration of the CP- method. The current electrode (C_1) is connected to the ore body and the remote electrode (C_2) is placed far outside the survey area. The colour indicates the strength of the charged potential above an ore-body. The dashed line shows the survey path along which the entire body will eventually be covered.

Self Potential (SP) is measured simultaneously with CP. SP is a natural potential in the ground created by electrochemical processes in connection with electronically conducting minerals (graphite, sulphides and oxides, Sato & Mooney (1960)). In

order to separate data from the two methods the current injected into the ore body is applied in pulses. SP is measured just before a current pulse while both CP and SP are measured during a current pulse. SP is not dependant on exposed graphite for current injection, and can be a very useful tool if there are several conductive bodies in the area of investigation.

SP may give negative potential values of 1000 mV or even more above graphite mineralisations. Measured SP signals less than 100 mV are not regarded as anomalies in mineral prospecting.

The equipment used for **combined CP and SP** measurements was developed at NGU in 2014. It consists of an immobile current transmitter and a mobile receiver (Voltmeter). The transmitter sends current between the ore electrode (C_1 in Figure 4.2) and the remote electrode (C_2 in Figure 4.2) and charges the ore body. The current is transmitted in pulses of two seconds on and two seconds off. The pulses are synchronized through GPS-time enabling the receiver to "know" when the ore body is charged. SP is measured when the current is switched off and CP+SP is measured with the current on, and then, in order to get the pure CP, SP is subtracted from the CP+SP measurement. All of this is done automatically during the measuring procedure. Each measurement is the potential between the two mobile electrodes. This means that every measurement has to be added consecutively to a total potential sum.

The position of each measured point is given by a GPS recorder at the position of the receiver. The accuracy of the positioning is +/- 5 m.



Figure 4.3: Establishing CP ore grounding point and data acquisition in combined CP and SP measurements.

4.1.3 2D resistivity and Induced Polarization (IP)

Detailed resistivity and Induced Polarisation (IP) sections give valuable information in the evaluation of graphite mineralisations.

Data acquisition

The 2D resistivity and IP methods are carried out by injecting current into the ground with the use of two electrodes and by measuring the voltage between two separate electrodes. Based on measured resistance (measured voltage / injected current) and a geometrical factor dependent on the electrode positions, the apparent resistivity and IP effect can then be calculated.

The 2D resistivity/IP measurements were performed using the Lund cable system (Dahlin 1993) and the instrument ABEM Terrameter LS (ABEM, 2012) was used to acquire data. As seen in Figure 4.4 four multi-electrode cables can be used, and for the surveys presented in this report, a Multiple Gradient electrode configuration (Dahlin & Zhou, 2006) was applied. Once the electrodes are connected to the ground and the measuring instrument, an automatic measuring procedure starts transmitting current at one electrode pair and measures electric potential at up to four electrode pairs simultaneously. Resistivity is measured when current is on while IP-effect is measured shortly after current break. An electrode separation of 2 m was used for the two profiles giving a maximum depth range of about 25 m. The resolution decreases with depth and resistivity data deeper than ca. 20 m are, by experience, of low reliability.

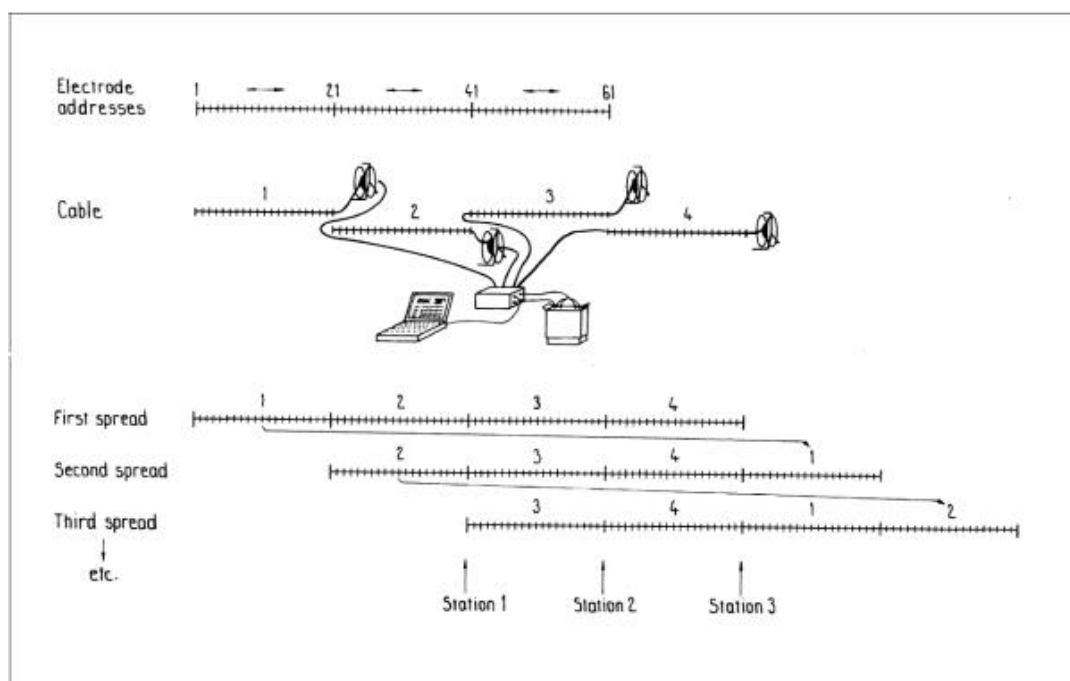


Figure 4.4: Diagram of measuring procedure illustrating the setup of the Lund System and the roll-along method for performing as many measurements as required. From (ABEM, 2012).

Quality of the data

The quality of 2D resistivity/IP data is dependent on current strength, resistivity in the ground and noise level in the area. We conclude, in general, that the quality is good, but some data have a too high standard deviation during inversion according to the software's guidelines. These data points were removed from the dataset in the inversion. Table 4.3 describes the number of deleted data points and remaining points for the final inversion. An alternative method to evaluate data quality is by looking at the absolute error in the inverted sections. Absolute error of less than 5 % is very good; 5 – 10 % is good; between 10 and 30 % is not that good but acceptable.

Table 4.3: 2D resistivity/IP. Number of measured, removed and remaining data points for inversion.

Name	Location	Measured data points	Removed data points	Final data points
Profile 1	Hesten	1168	226	942
Profile 2	Vardfjellet	1168	301	867

Data inversion

Almost all resistivity and IP measurements give an apparent resistivity and IP value. The apparent values represent a weighted average resistivity which resulted from resistivity of each heterogeneous volume in the surroundings of the measurement points. The data are inverted in order to find the specific resistivity of each part of the heterogeneous investigated volume. This is done by dividing the profile into blocks each characterized by specific resistivity values; these are adjusted following an iterative procedure until a theoretical model fits the measured data.

Resistivity measurements were inverted using the computer program RES2DINV (Loke, 2014) with robust data constraint.

Interpretation

Graphite is an electronically conducting mineral, and the resistivity in massive graphite ore bodies is commonly less than 2 Ωm , with conductivity higher than 500 mS/m, (Dalsegg (1994), Rønning et al. (2012), Rønning et al. (2014)). This can be used to distinguish between resistivity anomalies caused by graphite mineralisations and other ionic conducting geological materials such as porous rock filled with saline water, marine clay deposits and even sulphide deposits (resistivity less than 10 Ωm). Unfortunately, 2D resistivity/IP measurement may be disturbed by artificial conductivity effects interfering with responses from two or more sub-vertical conducting graphite structures (Rønning, et al., 2014).

Induced Polarization (IP) responds to electronic conducting minerals which are not in electrical contact. This means that massive graphite deposits should not give an IP

effect except for at the surface of the mineralisation. IP effects are often seen in the contacts between graphite bodies and surrounding host rock where graphite grains are not connected.

4.2 Geological methods

The investigated area is partly soil covered, but there are numerous outcrops particularly on the mountain tops. We sampled the graphite schist when found in these area and coordinates for every sampling points were recorded, taking care to obtain as representative samples as possible and from as large an area as possible. Usual samples size was about 1-2 kg. The samples were analysed further at the NGU laboratory.

Analytical methods

Samples from different outcrops were crushed using standard methods. The powders were analyzed for total carbon (TC) and total sulphur (TS) using a Leco SC-632 analyzer. The detection limits are 0.06 % and 0.02 % for carbon and sulphur respectively. The analytical uncertainty at 2 σ level is +/-15 % relative. The aggregate results for all samples are shown in Appendix 1 and are also reported under each area description in chapter 7.

The graphite industry uses the term "graphitic carbon" (Cg) when reporting graphite occurrences. This type of analysis is essentially the same as "total organic carbon" (TOC) but includes an extra step in which inorganic carbonate minerals and organic matter are removed by the use of acid and by roasting the sample before using a Leco carbon analyzer. In rock types with little or no carbonate minerals and organic matter, analyses of total carbon (TC) would be similar or close to TOC and graphitic carbon (Cg) but the former is much cheaper and faster. The commercial laboratory procedures for TC, TOC and Cg analyses are described by, e.g. www.alsglobal.com

A number of standard thin sections were made from different occurrences. The modal content of graphite in the thin sections was measured using the ZEN 2 pro program from Zeiss.

4.3 Aerial photogrammetry

The structural geology at Hesten and Vardfjellet were studied by Henderson & Kendrick (2003). Lately, NGU has developed techniques to create 3 D models of the geology which might be beneficial for the graphite project on Senja.

The work process to come from 2D images to an integrated 3D topographic-geological model is rather long and the systematic method has been developed at NGU during the time span of this project. This process shall only be briefly summarized here and is shown visually in Figure 4.5.

4.3.1 Equipment

We use a DJI Phantom 4 drone (Figure 4.6) which is equipped with a control unit driven from an Ipad and the *Litchi* application (Figure 4.7).

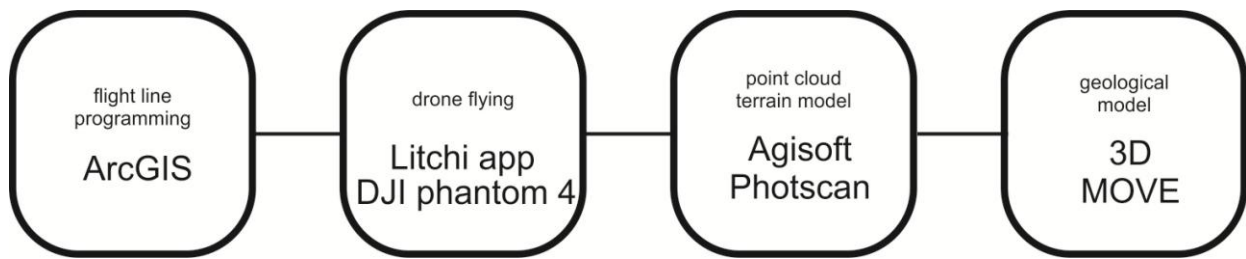


Figure 4.5: Summary of the workflow process developed at NGU to construct 3D topographic-geological models from aerial photos.



Figure 4.6: The drone used to acquire GPS-rectified images from the air- the DJI Phantom 4.



Figure 4.7: The control unit for the DJI Phantom 4 drone with accompanying Ipad. This is used to remotely control the drone with the *Litchi* application.

The principal of building 3D topographic models from 2D images taken from the air is relatively simple and well-documented and is used many places in the world. 'Structure from motion' describes the process in which advanced software programs compare identical pixel values in adjacent photos with at least 60 % of overlap (Figure 4.8). There exists many such software programs on the market to make such 3D models and we have chosen *Agisoft Photoscan Professional*. When this process is undertaken on many points over a number of different images, the software is able to calculate both the distance to the individual pixels in the topography to the drone camera and the distance and angle to each individual point in the topography from other points. From this a point cloud of the topography is constructed (Figure 4.11 A-D) which is the foundation for a wireframe mesh which is the basis for the elevation model. Afterwards the detailed orthophotos can be draped onto the elevation model.

A minimum 60 % overlap of the images is essential to the construction of a continuous, high quality model. In Norway, where a highly variable topography is present, it is therefore necessary to vary the drupe the terrain while it is flying to maintain overlap. It is therefore highly desirable or even essential to include pre-programmed XYZ points into the drone flight-plan before acquisition. We achieve this with an in-house, tailor-made toolbox in ArcGIS which is called *Flightplanner* (see Figure 4.9) From a 2D shapefile over the target area a XYZ.csv file is created which is directly transferred to the Litchi-application on the Ipad for uploading to the drone (Figure 4.10).

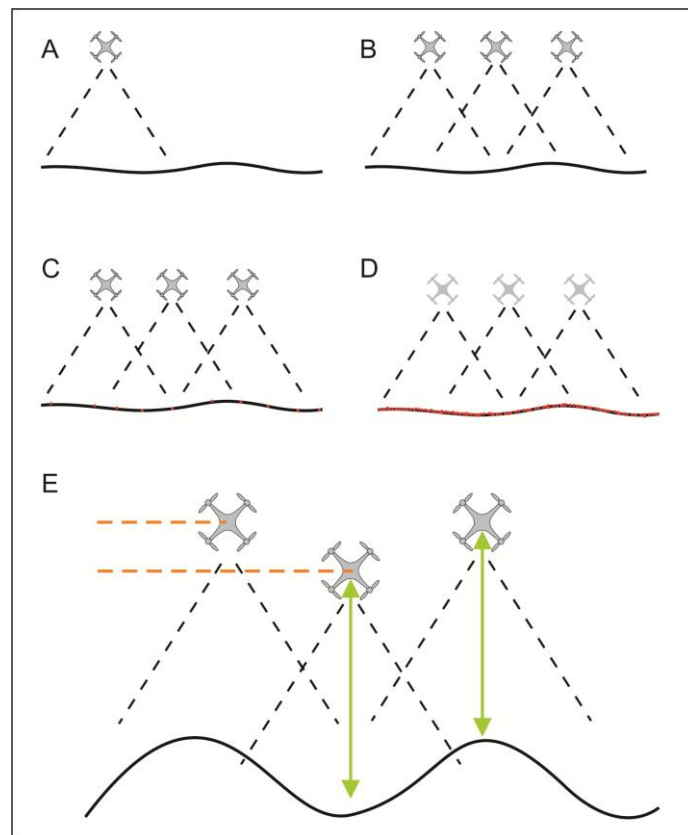


Figure 4.8: The principal of construction of a 3D elevation model from 2D static images taken from a drone.

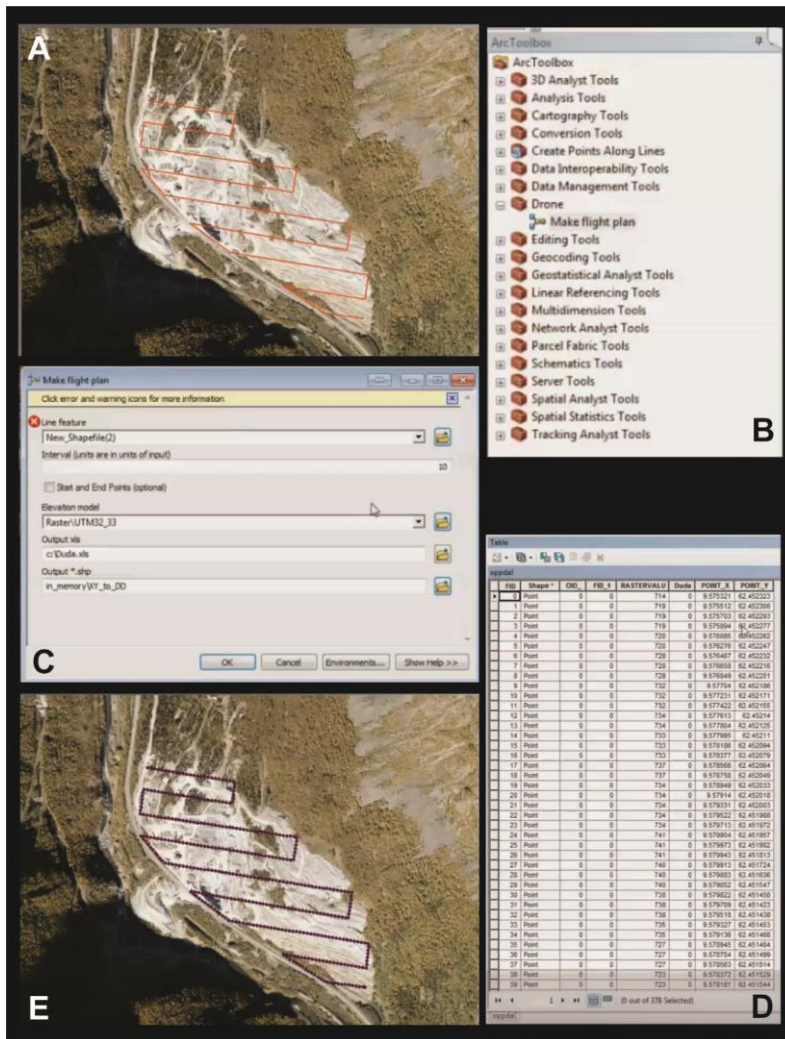


Figure 4.9: Automatic flight-plan construction in ArcGIS. This produces a .csv file with XYZ points that can be uploaded to the drone.

The image shows the Litchi application interface. The main map displays a mission plan for a drone at 'Fauske Marmor 1 (Østre, 90) - 2.1km | 14min'. The mission is represented by a series of numbered points (1-99) connected by lines, forming a circular path around a central point. The settings panel on the right is open, showing the following configuration:

- Latitude: 67.2856597780742
- Longitude: 15.36883234977222
- Altitude: 30m
- Ground Elevation: 57m (0m below first waypoint)
- Speed: Cruising
- Curve Size: 0m
- Heading: 314°
- POI: None
- Gimbal Pitch: Disabled
- Actions: 2
 - Tilt Camera: -90°
 - Take Photo

Figure 4.10: Image from the Litchi application which controls the drone automatically in the air.

Figure 4.11 shows 187 photos from the Vardfjellet deposit uploaded to the *Agisoft Photoscan Professional* software to begin constructing the point cloud model. Figure 4.11A shows the first point cloud, also called a light point cloud. The GPS determined camera positions and pictures are shown with blue triangles. Subsequently, the software creates a dense point cloud (Figure 4.11B). From this dense point cloud an elevation wireframe is constructed which is shown in Figure 4.11C. Finally, the GPS rectified images are draped over the elevation model (Figure 4.11 D).

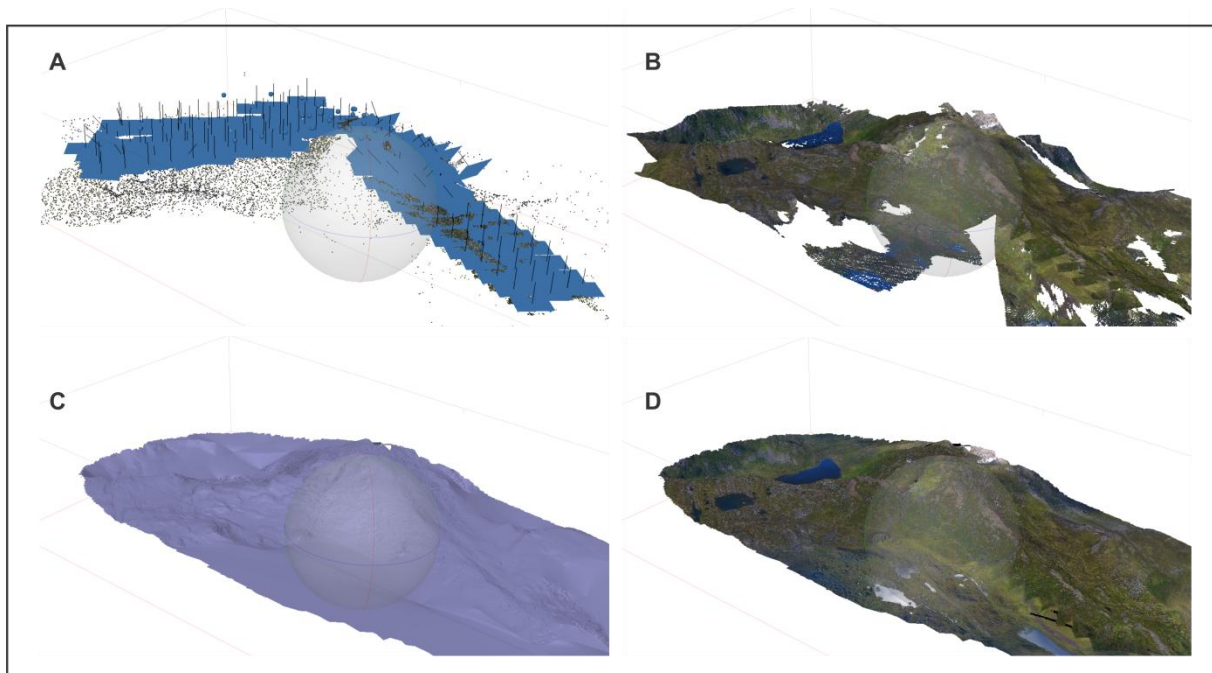


Figure 4.11: Construction of the elevation model with the software *Agisoft Photoscan Professional* from Vardfjellet. A: Images uploaded to the software. The images are shown in blue. This 'light' point cloud has over 40 000 points. B: dense point cloud. The calculated points are so dense that they begin to look like a surface. The software program has calculated over 15 million points. C: elevation model created from the dense point cloud. Here there are over 1 million surfaces. D: Finished elevation model with images.

5. SELECTION OF FOLLOW-UP OBJECTS

Figure 5.1 shows calculated apparent resistivity from the helicopter-borne electromagnetic measurements using the coaxial 7001 Hz frequency (from Rodionov et al. 2014). Red/violet colours show low apparent resistivity (good electrical conductivity) which may be caused by graphite mineralisations.

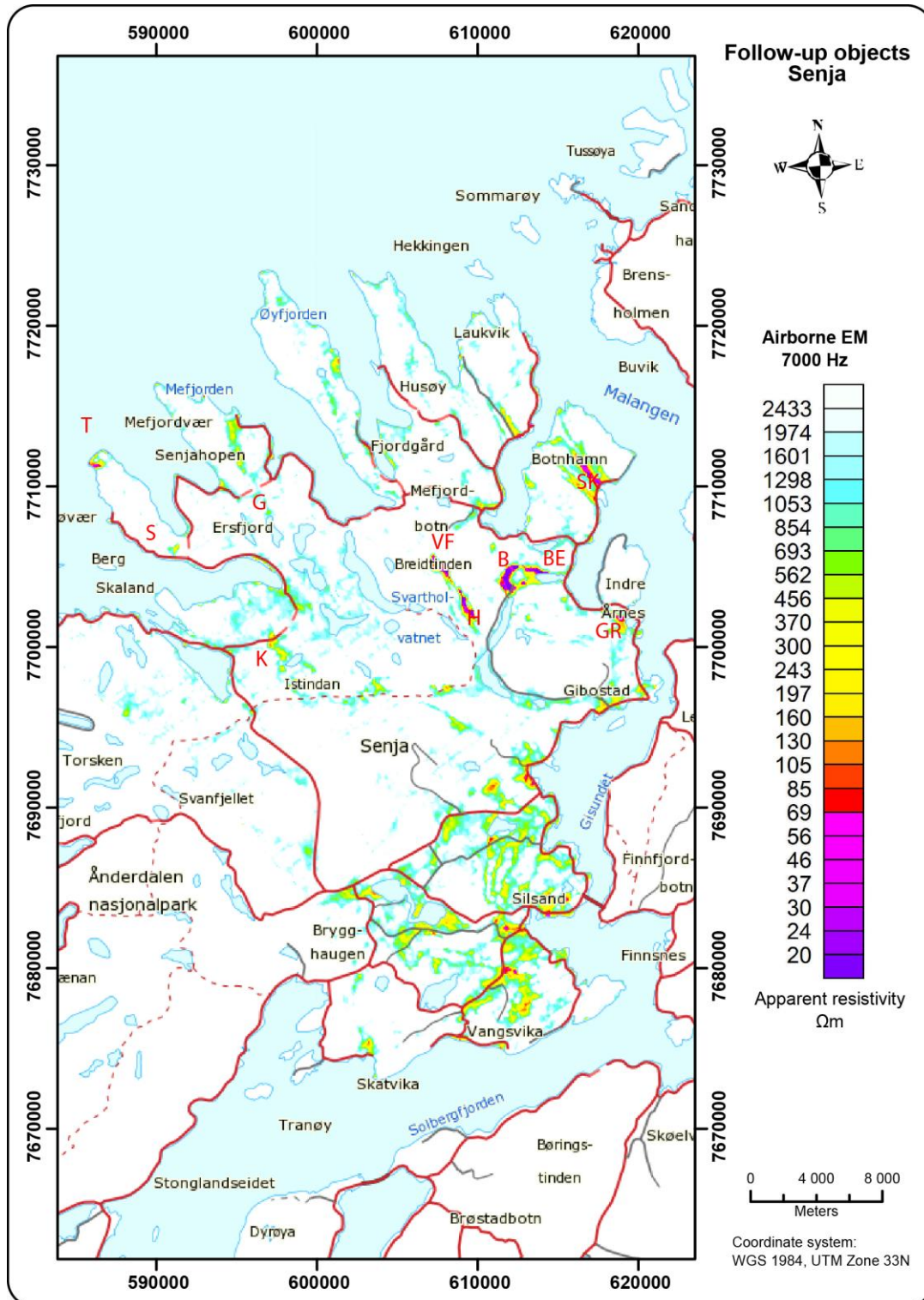


Figure 5.1: Apparent resistivity (7001 Hz) and graphite mineralisations on Senja. T= Trælen, S= Skaland, G= Geitskaret, K= Krokeldalen, SK= Skarsvåg, VF= Vardfjellet, H=Hesten. B=Bukken, BØ= Bukken East and GR= Grunnvåg.

The Trælen and Skaland deposits are well known especially from mining activities and also from follow-up work (Dalsegg 1986, Rønning et al. 2012). The two showings called Geitskaret and Krokeldalen have previously been investigated with ground geophysics (Dalsegg 1985). At the Skarsvåg showing, there is a mineralisation of sulphides and some graphite, and this was found to be sub-economical. The most pronounced electromagnetic anomalies from the helicopter-borne geophysics are at Hesten, Vardfjellet, Bukkemoen, Bukkemoen East and Grunnvåg. The Bukkemoen showing has partly been investigated with ground geophysics before (Lauritsen 1988). In this area, two conductive structures, probably graphite, can be followed for ca. 1 km in the N-NE direction from Lysvatnet. Detailed studies showed that these could consist of several parallel graphite lenses.

In the southern part of the area covered by helicopter-borne geophysics, several low resistivity anomalies are shown. In this area, we observed a granitoid intrusive (see Figure 5.1) and therefore high quality graphite mineralisations are less likely.

The apparent resistivity calculated from helicopter-borne measurements has low resolution, and to be able to evaluate the quality and quantity of individual graphite mineralisations ground follow-up investigations are necessary. Based on these discussions, the areas called Hesten, Vardfjellet, Bukken (Bukkemoen), Bukken East and Grunnvåg (see Figure 5.2) were selected for follow-up work in co-operation with the Troms County administration.

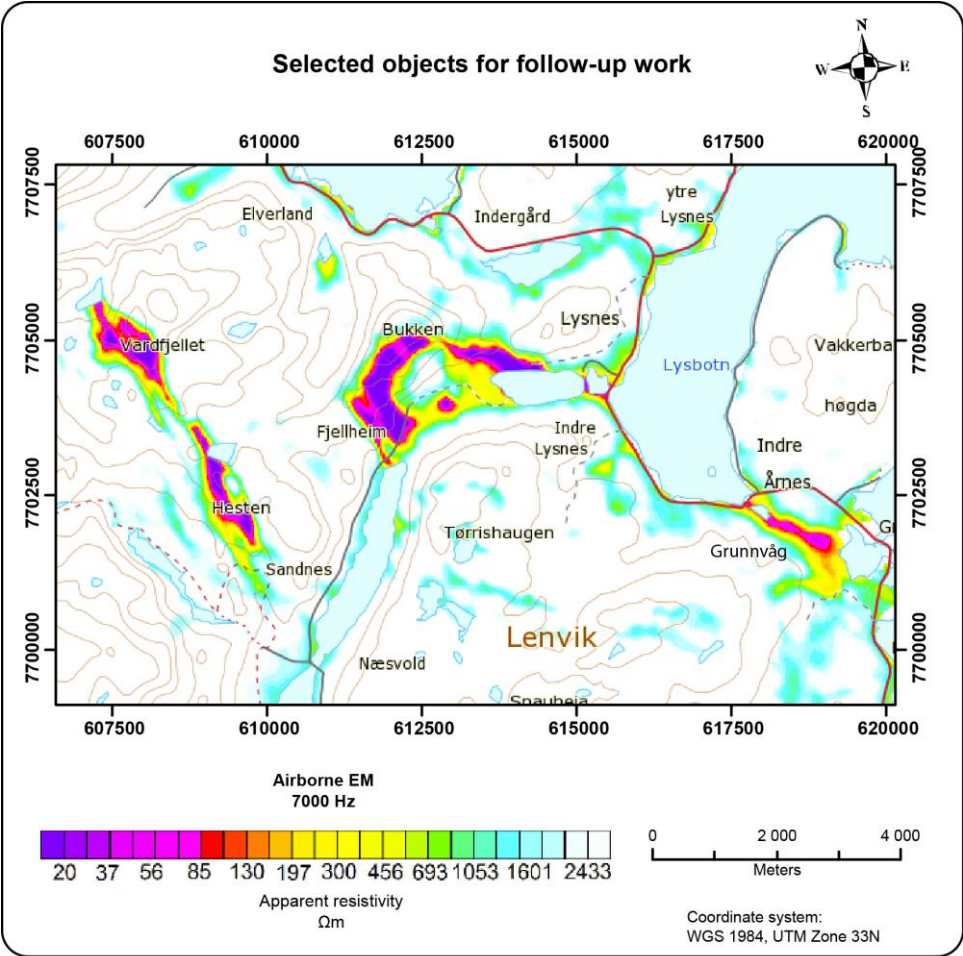


Figure 5.2: Apparent resistivity anomalies proposed for follow-up investigations on Senja, Vardfjellet, Hesten, Bukken and Grunnvåg.

6. RESULTS OF GROUND GEOPHYSICAL INVESTIGATIONS

Ground geophysical investigations were performed as planned at Hesten and Vardfjellet in August 2016.

6.1 Geophysical results, Hesten

The apparent resistivity anomaly from helicopter-borne EM measurements at Hesten is shown in figure 6.1. The anomaly can be followed for ca. 2 km and the width is up to ca. 300 m. The apparent resistivity is partly less than 20 Ωm which may be caused by graphite.

At Hesten, we performed Charged Potential (CP) in combination with Self Potential (SP) measurements and one profile of 2D resistivity in combination with Induced Polarisation (IP). Location of CP grounding and the resistivity/IP profile is shown in figure 6.1.

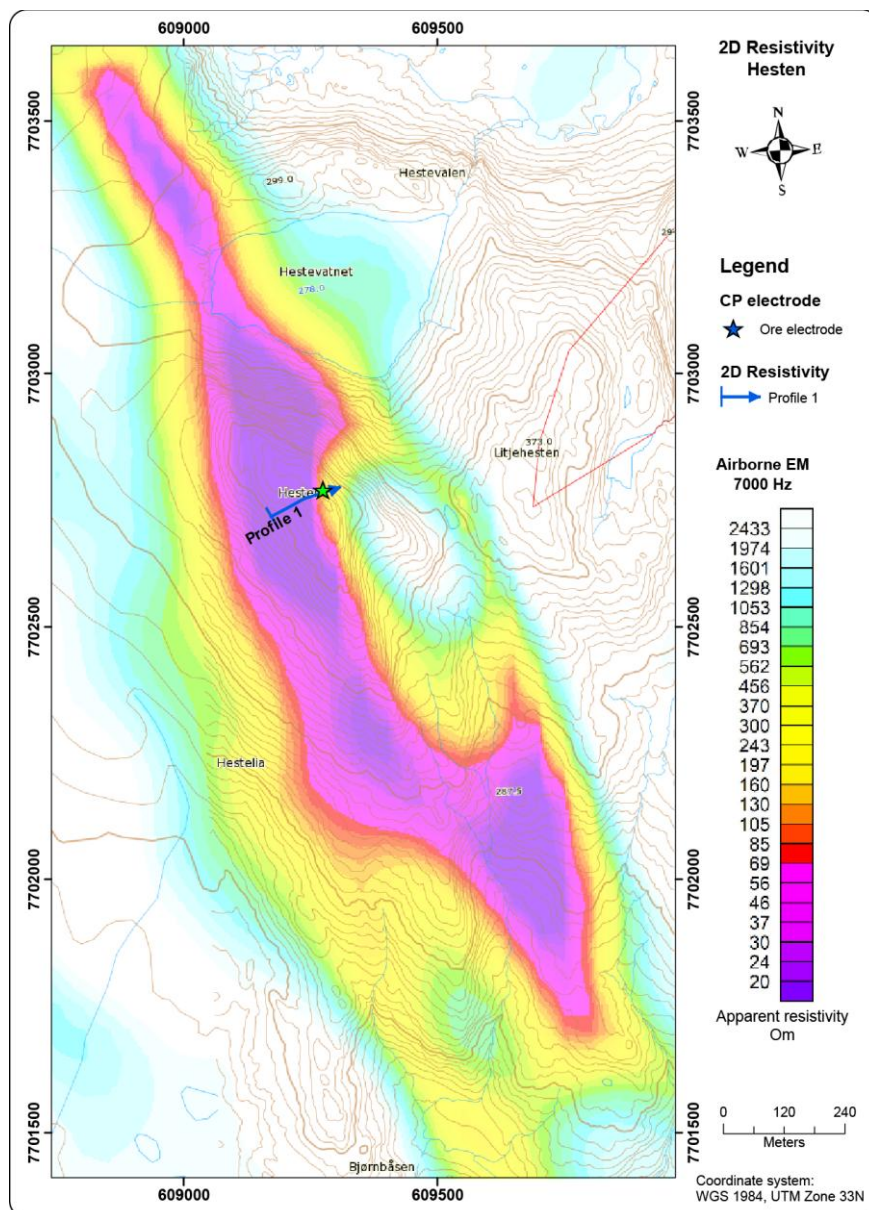


Figure 6.1: Apparent resistivity calculated from 7001 Hz coaxial coils at Hesten. Location of CP grounding point and 2D resistivity/IP profile is given as green star and blue line respectively.

6.1.1 CP measurements at Hesten

In the Hesten area, we performed CP measurements with one ore grounded electrode. Technical details are given in table 6.1.

Table 6.1: Coordinates (WGS 84, UTM Zone 33), applied current and no. of measured points used for CP measurements at Hesten. R1 is the remote electrode.

Electrode	X-coordinate	Y-coordinate	Current (A)	No. of measurements
1	609274	7702770	1,0	123
R1	610632	7703905		

During the measurements, two receivers were used, but there appears to be an error on the CP data for one of them. We tried to recover the data, but it was impossible to get reliable data. Due to this, only data from the working receiver are presented in Figure 6.2.

Characteristic for this CP contour map are red colours at the grounding electrode (electrode effect), a large area with constant potential shown in green and the blue area to the east.

The electrode effect is standard and does always show up representing a potential drop immediately outside the ore electrode.

The green area is of interest. Inside this area the charged potential is at a constant level (ca. 28 mV). No potential drop indicates a good electrical contact between conducting structures within the area. The superimposed SP data indicate several conductors (see next chapter) but it is not possible to resolve the individual conductors with CP. From this we can conclude that electrically connected graphite is present in a total length of more than one km and in a total width of at least 250 m. It is probable that graphite is in electrical contact within the entire helicopter-borne EM anomaly in a total length of ca. 2 km. We can also conclude that despite the presence of several graphite exposures, grounding in these will give the same image.

The blue area in Figure 6.2 represents the host rock potential level. From the graphite mineralisation (green area) to this level there is a potential drop of ca. 28 mV. This potential drop could be used to interpret the depth extent of the graphite structure at Hesten (Kihle & Eidsvig 1978). Since we do not have full coverage of CP data over the entire mineralisation, and that we were not able to find the host rock resistivity (see 2D Resistivity/IP interpretation), this calculation cannot be made. However, there are indications (the low potential drop of 28 mV) that the depth extent is in the order of several hundreds of meters.

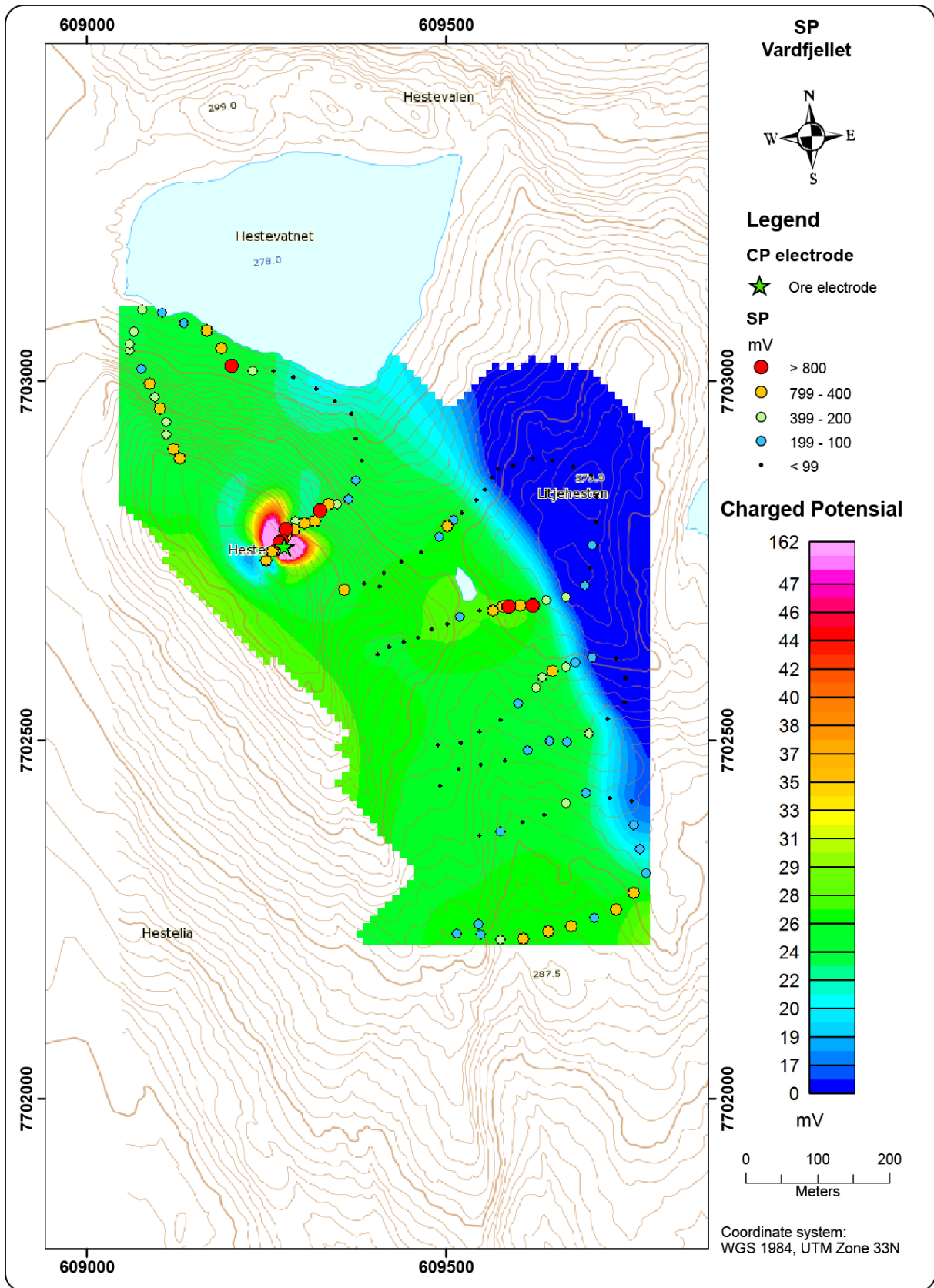


Figure 6.2: Results of CP measurements at Hesten with SP anomalies superimposed. The measured CP measuring points are the same as SP points.

6.1.2 SP measurements at Hesten

SP measurements at Hesten were performed simultaneously with CP measurements. The results are shown in figure 6.3.

As a standard, we used an electrode separation of ca. 30 m. To obtain a better resolution, this was decreased to ca. 10 m in anomalous areas. Figures 6.3 show numerous SP anomalies higher than 800 mV and also some more moderate values. SP anomalies as high as 800 mV indicate graphite mineralisations, which are also observed at several locations in the area (see Figure 6.4). Lower anomalies can also be caused by graphite.

Most of the high SP anomalies represent individual graphite structures with less conducting material in between. This pattern indicates several parallel graphite horizons. All of the high anomalies lie within the low apparent resistivity area from helicopter-borne EM measurements confirming the power of these methods to delineate graphite horizons.

In figure 6.4 we plot SP-anomalies on top of the geological map from Henderson & Kendrick (2003). Most SP-anomalies coincide with graphite bearing rocks. However, several SP-anomalies fall outside of the known graphite zones, and even in the acidic gneiss areas we find strong SP anomalies. The discrepancies are probably caused by inaccurate background mapping without GPS (Henderson & Kendrick, 2003). This mapping was carried out at a scale of 1:5.000, but was performed on an enlarged topographical map at 1:50.000.

Unfortunately, there is a lack of SP data in both ends of the EM anomaly. However, it would be expected that graphite mineralisations would follow the helicopter-borne EM anomalies.

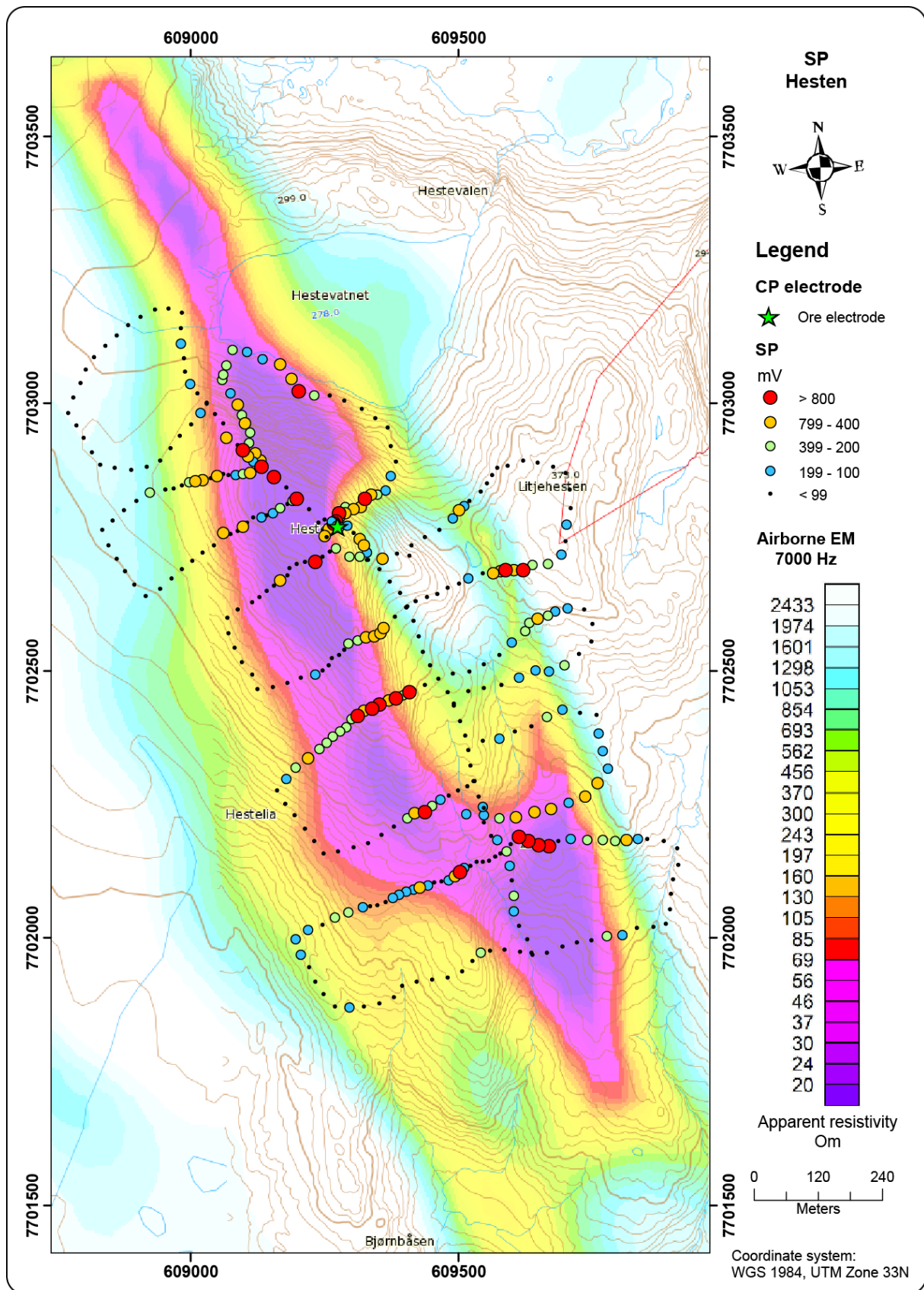


Figure 6.3: Results of SP measurements at Hesten on top of apparent resistivity from helicopter-borne EM measurements (7001 Hz, from Rodionov et al. 2014).

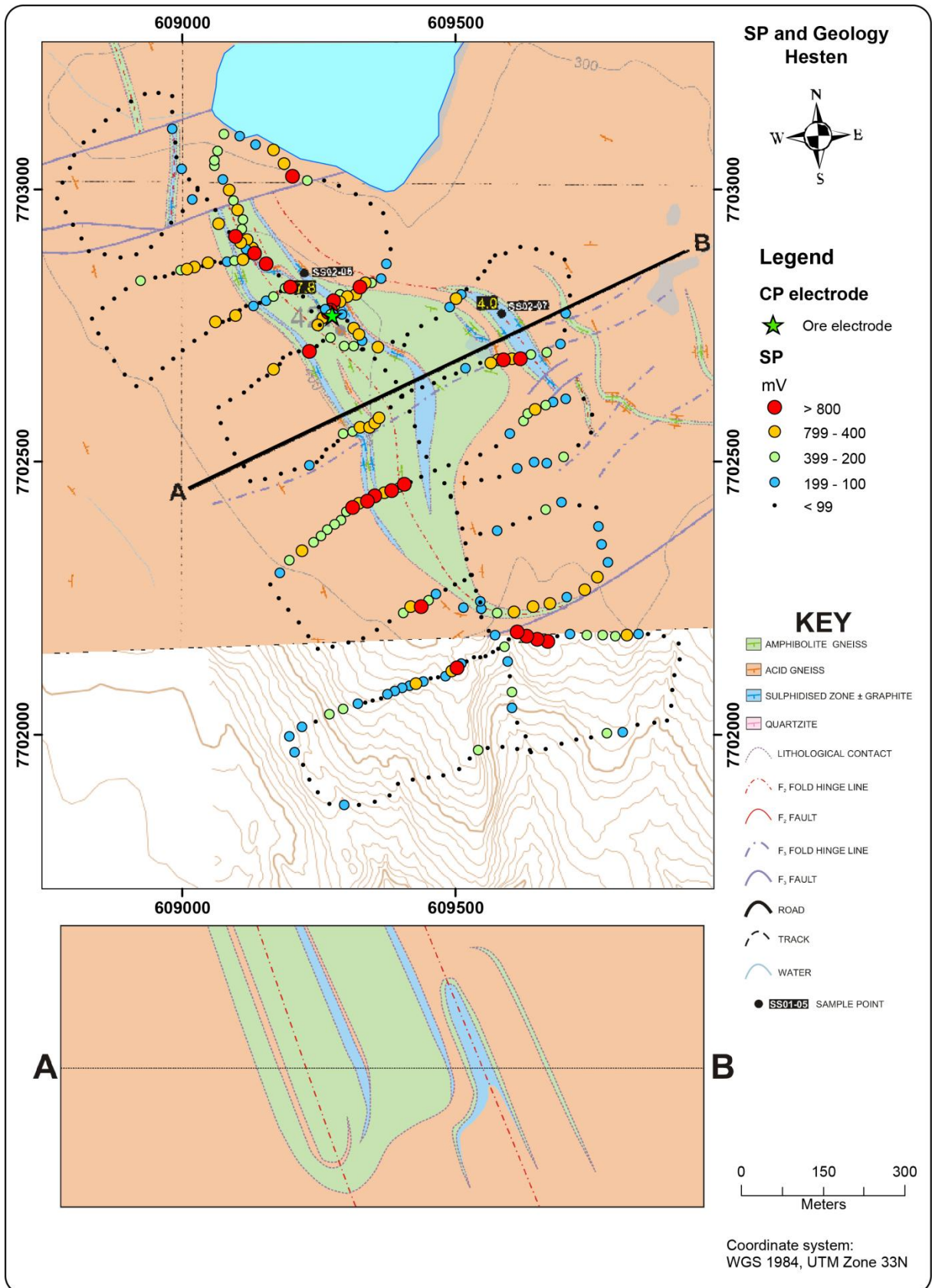


Figure 6.4: SP anomalies at Hesten superimposed at geological map modified from Henderson & Kendrick (2003). Cross section is not to scale.

6.1.3 2D Resistivity/IP at Hesten

At Hesten, one 2D Resistivity/IP profile was measured just south of Hestevatnet (See Figure 6.1). The results are presented in Figure 6.5.

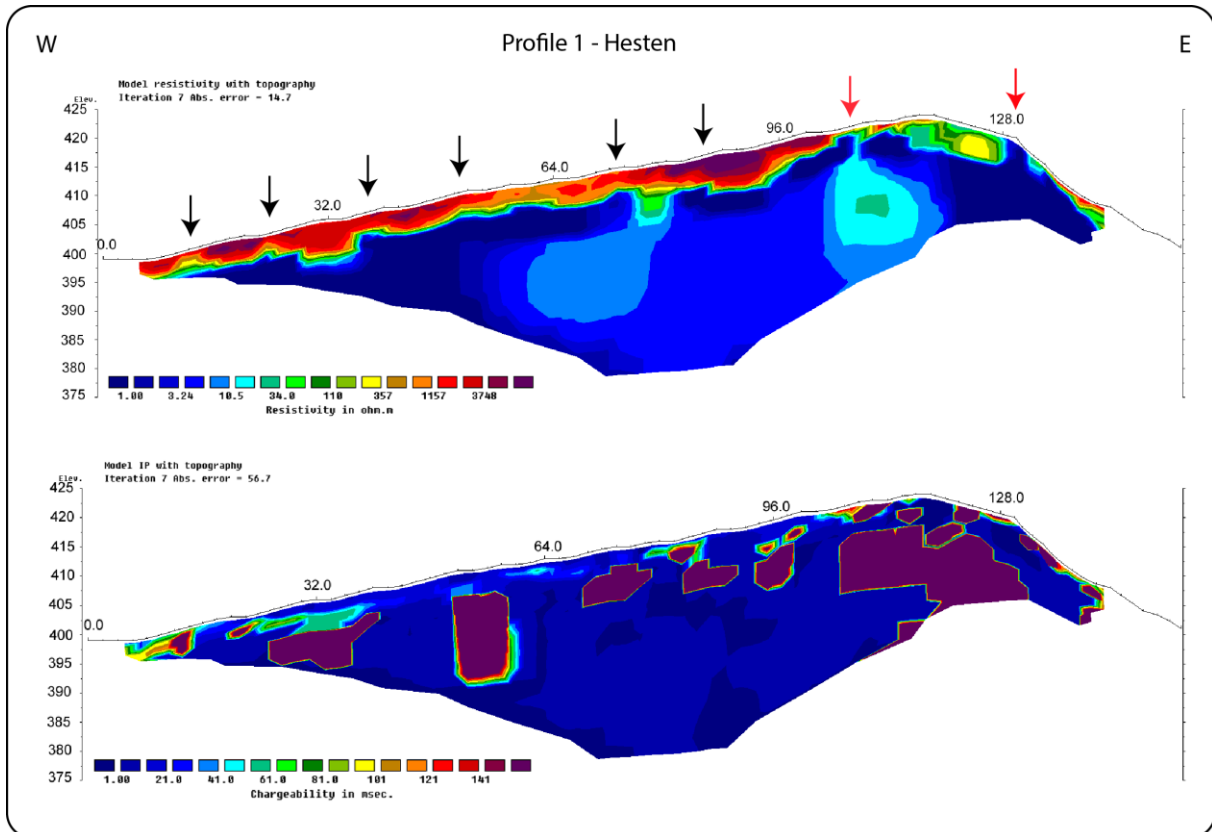


Figure 6.5: 2D resistivity (top) and IP (bottom) results along profile 1 at Hesten. Known graphite outcrops are indicated with red arrows, possible (interpreted) graphite zones with black arrow.

Along this line, graphite could be observed at two locations (red arrows in Figure 6.5). Low resistivity ($<3 \Omega\text{m}$) can be observed along the entire profile. This might be an indication of continuous graphite. However, modelling has shown that several individual graphite zones might explain such a pattern (Rønning et al. 2014). Based on the near surface resistivity pattern, we can interpret a number of conducting zones that probably are graphite. Due to the mixed responses, it is impossible to interpret the thickness of the individual zones except for the two outcropping zones that appear to be 3-4 m thick.

Very high IP anomalies confirm that graphite mineralisations can occur along the entire profile.

Based on the resistivity/IP measurements we can conclude that graphite zones with a thickness of more than 160 m (total length of the profile) are more than likely present. Unfortunately, this can be made up of several zones. Thickness of two of these appears to be 3 - 4 m. The potential for valuable graphite is quite large in the Hesten area.

6.2 Geophysical results, Vardfjellet

The apparent resistivity anomaly from helicopter-borne EM measurements with frequency 7001 Hz at Vardfjellet is shown in figure 6.1. The anomaly can be followed for ca. 2 km and the width is up to ca. 480 m. The apparent resistivity is partly less than 20 Ωm and this low resistivity might be an indication of graphite.

At Vardfjellet, we performed Charged Potential (CP) in combination with Self Potential (SP) measurements and one profile of 2D resistivity in combination with Induced Polarisation (IP). The location of CP grounding and the resistivity/IP profile are shown in figure 6.1.

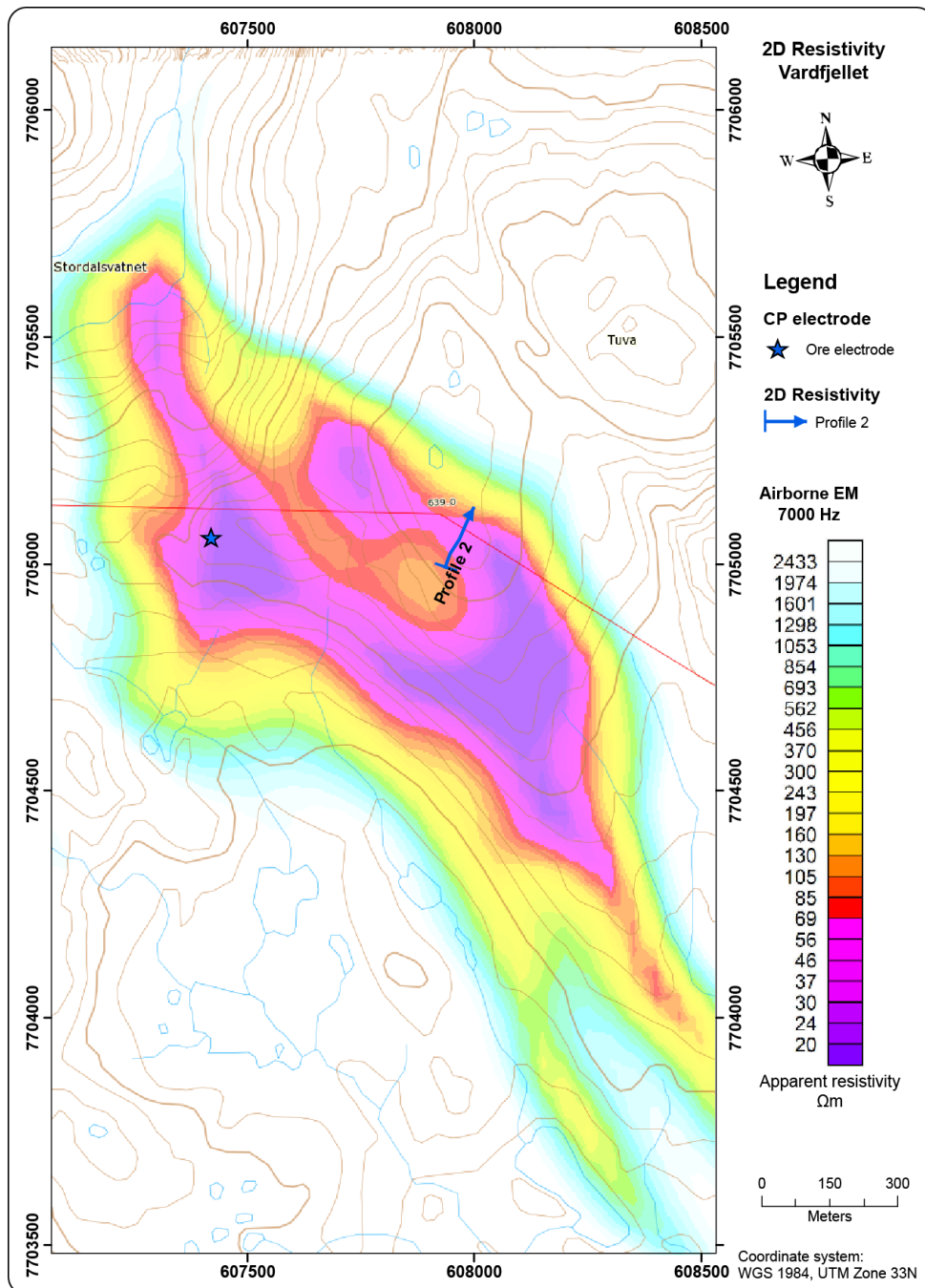


Figure 6.6: Apparent resistivity calculated from 7001 Hz coaxial coils at Vardfjellet. Location of CP grounding point and 2D resistivity/IP profile is given as green star and blue line.

Technical details of the CP measurements are given in table 6.2.

Table 6.2: Coordinates (WGS 84, UTM Zone 33), applied current and no. of measured points used for CP measurements at Vardfjellet. R2 is the remote electrode.

Electrode	X-coordinate	Y-coordinate	Current (A)	No. of measurements
1	607421	7705059	1,0	267 + 160
R2	606274	7704738		

Due to bad weather, which caused instrumental problems, the quality of the CP data at Vardfjellet was not trustworthy, and hence no data are presented here. However, the measured data indicate electrical contact between the different graphite horizons, but it is impractical to delineate the form of individual graphite bodies.

6.2.1 SP measurements at Vardfjellet

SP measurements at Vardfjellet were performed simultaneously with the CP measurements. The results are shown in figure 6.7.

As a standard, an electrode separation of ca. 30 m was used. To obtain a better resolution, this was decreased to ca. 10 m in anomalous areas. Figure 6.7 shows numerous SP anomalies higher than 800 mV and also some more moderate values. SP anomalies as high as 800 mV indicate graphite mineralisations. Graphite is also observed outcropping at several locations in the area (see Figure 6.8). Lower anomalies can also be caused by graphite.

Most of the high SP anomalies represent individual graphite structures with less conducting material in between. This pattern indicates several parallel graphite horizons at Vardfjellet. All the high anomalies lie within the low apparent resistivity area from helicopter-borne EM measurements, confirming again the power of these methods to delineate graphite horizons.

In figure 6.8 the SP-anomalies are plotted on top of the geological map from Henderson & Kendrick (2003). Most SP-anomalies coincide with graphite bearing rocks. However, several SP-anomalies fell outside the known graphite zones, and even in the acidic gneiss areas we find strong SP anomalies. As for the Hesten area, these discrepancies are probably caused by inaccurate background map during geological mapping (Henderson & Kendrick, 2003). This mapping was undertaken at a scale of 1:5.000, but was performed on an enlarged topographical map in scale 1:50.000. No GPS system and GIS software were available and the accuracy of the mapping was not sufficient.

Unfortunately, there is a lack of SP data in both ends of the EM anomaly. However, graphite mineralisations are expected to follow the helicopter-borne EM anomalies.

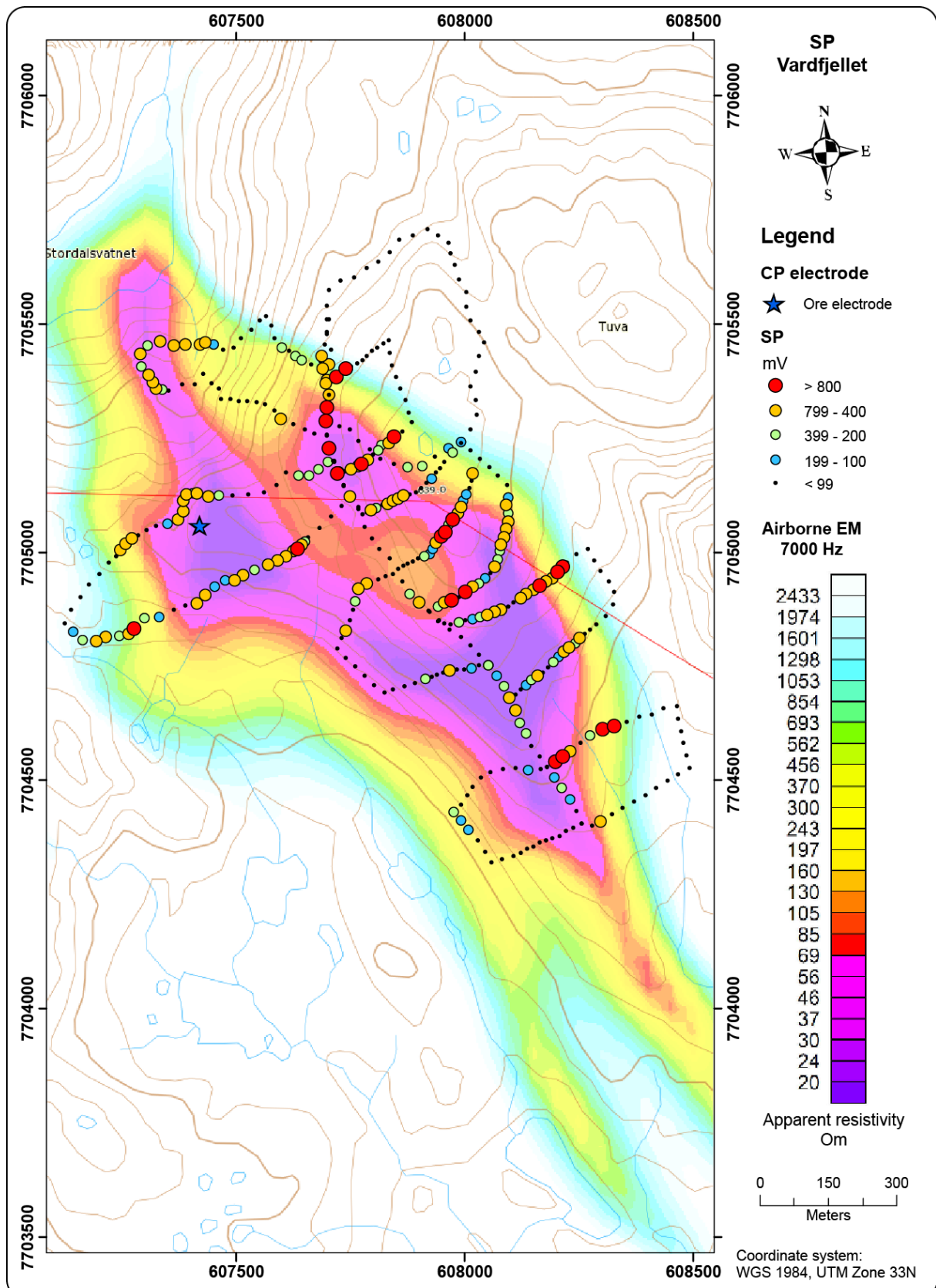
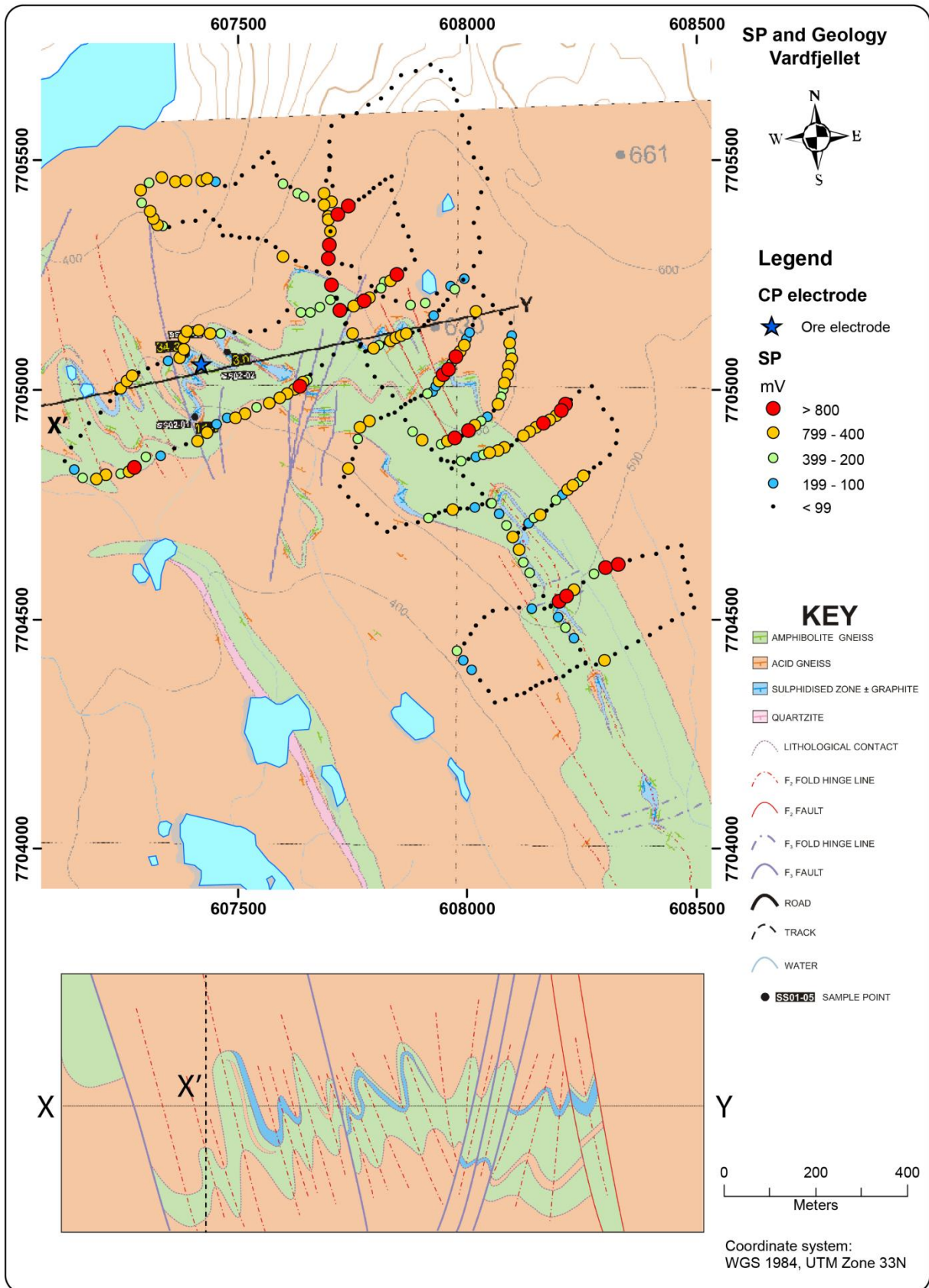


Figure 6.7: Results of SP measurements at Vardfjellet superimposed on apparent resistivity (7001 Hz, from Rodionov et al. 2014).



6.2.2 2D Resistivity/IP at Vardfjellet

At Vardfjellet, one 2D Resistivity/IP profile was measured just S of the Vardfjellet 639 m.a.s.l. summit crossing the path to the summit (See Figure 6.7). The results are presented in Figure 6.9.

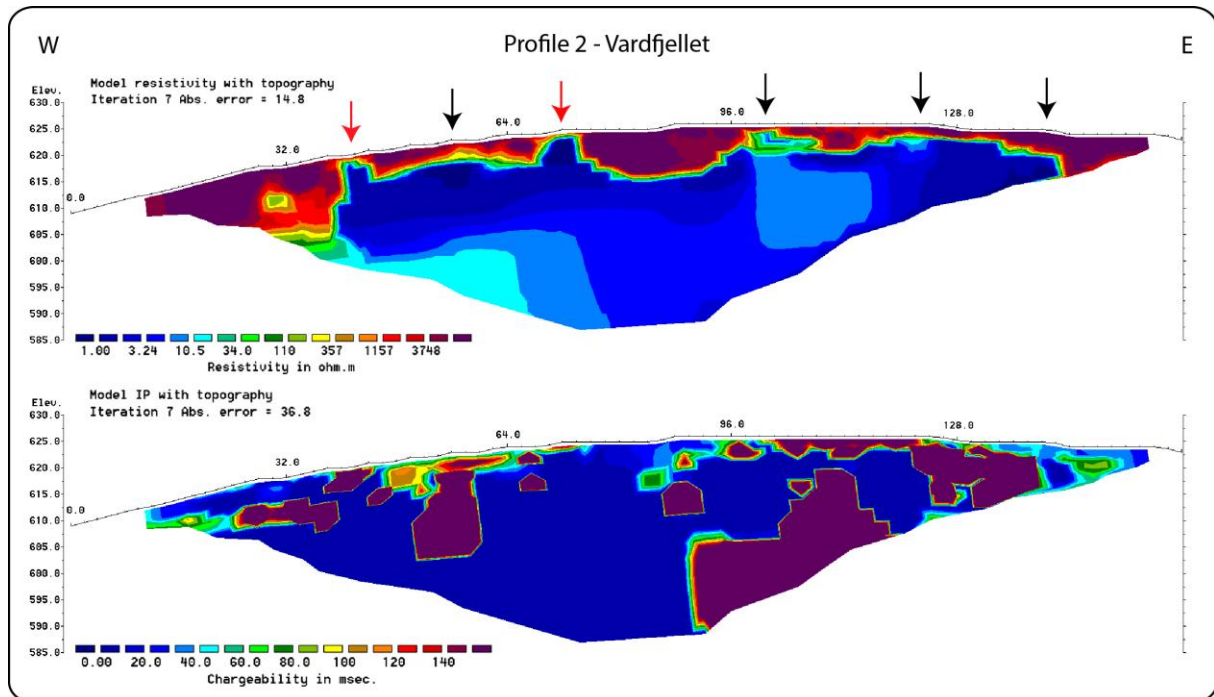


Figure 6.9: 2D resistivity (top) and IP (bottom) results along profile 1 at Vardfjellet. Known graphite outcrops are indicated with red arrows and possible (interpreted) graphite zones are shown with a black arrow.

Also along this line, graphite could be observed at two locations (red arrows in Figure 6.9). Partly low resistivity ($<3 \Omega\text{m}$) can be observed at a length of ca. 100 m along the profile, indicating graphite. High resistivity ($> 5000 \Omega\text{m}$) in both ends of the profile represents the granitic host rock. However, modelling has shown that the resistivity pattern in the central part of the profile is typical for individual (sub-)vertical graphite zones (Rønning et al. 2014). Based on the near surface resistivity pattern, a number of conducting zones can be interpreted (black arrows in Figure 6.10) that are probably caused by the presence of graphite. Due to the nature of the responses, it is impossible to interpret the thickness of the individual zones except for the two outcropping zones that appear to be 3-5 m thick. As can be seen in Figure 6.6, this 2D resistivity/IP profile covers less than half of the helicopter-borne EM anomaly, and the potential for valuable graphite is quite large in the area.

Very high IP anomalies confirm that graphite mineralisations are present along a large part of the profile.

Based on the resistivity/IP measurements we can conclude that graphite zones are most likely present in a horizontal thickness of ca. 100 m, but this line covers less than half of the helicopter-borne EM anomaly (see Figure 6.6). Unfortunately, this can be several smaller graphite zones. Thicknesses of two of these appear to be 3-5 m. The potential for valuable graphite is quite large in the Vardfjellet area.

7. RESULTS OF GEOLOGICAL INVESTIGATIONS

Geological investigations were performed at Hesten, Vardfjellet and Grunnvåg in August 2016. In this chapter the results of geological mapping, sampling, chemical analysis, petrography and modal analyses of graphite are presented.

Appendix 3 presents the earlier structural map made by Henderson and Kendrick (2003) covering both Hesten and Vardfjellet (also shown in Figures 6.4 and 6.8 separately). The mapping was performed on paper based topographic maps, there is therefore some degree of error and mismatch compared to our present GPS based geophysical maps and sampling. The sulphidised units containing the graphite schists, contain on average less than 1% total sulphur.

7.1 Geological investigations at Hesten

On the upper part of the Hesten, outcrops of graphite schist can be found over a distance of about 1 km. The graphite occurs in a strongly foliated rusty, weathered graphite schist. The graphite appears partly enriched in individual layers and partly evenly distributed in the rock. Nowhere on Hesten is there possible to study the contact relationship between the graphite schist and the host rocks in detail. The mineralised zone has a variable and unknown width. However, from scattered outcrops, it is observed that along certain profiles minimum width perpendicular to the strike can be up to 150 meters. The geological map (Henderson & Kendrick 2003) is shown in Appendix 3. This shows that the graphite schist on the surface consists of several apparently isolated lenses that are isoclinally folded and refolded. For details on the structural geology the reader is referred to Henderson & Kendrick (2003).

Samples were collected on the exposed outcrops, in order to obtain as even a distribution as possible. The samples were analysed at NGU lab and the samples points are shown in Figure 7.1.

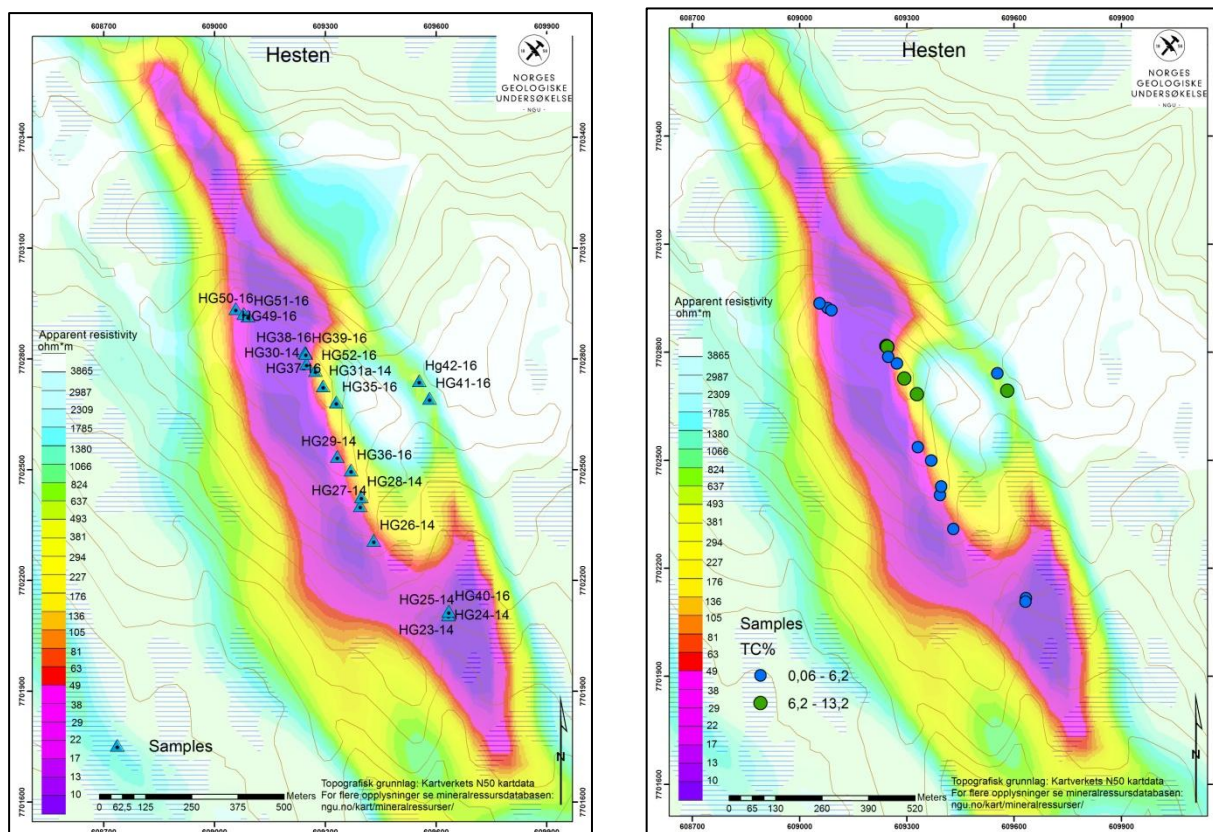


Figure 7.1: Graphite sampling points and analyzed graphitic carbon content at Hesten. The background is apparent resistivity calculated from frequency EM 7001 Hz (See Rodionov et al., 2014 for geophysical details).

Individual analyses of 21 samples collected at the mountain of Hesten are presented in Appendix 1. The average C_g content is 5.8 % with a maximum and minimum of 12.8 % and 1.7 %. The standard deviation is 3.0 %. This graphitic carbon content is comparable with content in deposits under development in Canada and Mozambique. In comparison with Vardfjellet (chapter 7.2) a narrower range in content of C_g is observed. The average sulphur content in these samples is 0.2 % with a maximum and minimum value of 0.85 % and 0.01 %.

7.2 Geological investigations at Vardfjellet

The Vardfjellet mountain is much better exposed than Hesten and graphite schist can be found outcropping over an area of 1.7 km in length and up to 350 meter in width. However, the helicopter-borne EM anomaly indicates graphite in a total length of ca. 2 km. From the outcrops it is evident that there are a number of apparently isolated minor outcrops that occur in the 1.7 km long mineralised zone.

The exposures of graphite schist occur mainly on the northern and western side of the mountain where scattered outcrops are found (see Figure 7.2). It is very rare to see contact relationships with the country rock except at some few localities (Figure 7.3). The graphite schist is part of a succession that comprises sulphide bearing quartz and feldspar rich rocks. At some localities, quartz is the dominating mineral and the rock would be classified as (sulphide and graphite bearing) quartzites.

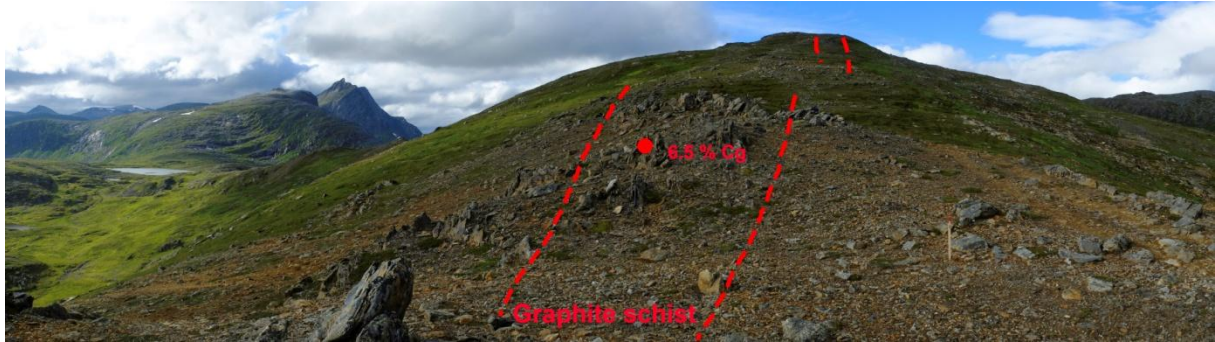


Figure 7.2: The southern side of Vardfjellet with some of the graphite lenses and sample point and analyses indicated. The total width of the graphite schist is ca. 7 m.



Figure 7.3: Rock face (about 150 m long) on the western side of Vardfjellet comprising a mixture of graphite schist and sulphide bearing quartz and feldspar rich rock. (sample points and analyses are indicated).

This succession is part of a rock association that comprises amphibolitic- and granitic (granodioritic) gneisses, that are intruded by several generations of granitic and pegmatitic dykes. Geological and structural mapping of Vardfjellet are shown in Appendix 3 and described by Henderson & Kendrick (2003). The Vardfjellet consists of a number of isolated lenses of graphite schist that are isoclinally folded and refolded and dissected by a number of minor faults.

Samples were collected on the exposed outcrop, in order to get as even a distribution as possible. The samples were analysed at NGU lab and the samples points are shown in Figure 7.4.

Individual analyses of 37 samples collected at Vardfjellet are presented in Appendix 1. The average Cg content is 9.2 % with a maximum and minimum of 40.3% and 1.1%. The standard deviation is 7.5 %. This graphitic carbon content is comparable with content in deposits under development in Canada and Mozambique. The average Sulphur content in these samples is 0.3 % with a maximum and minimum value of 1.3 % and 0.02 %.

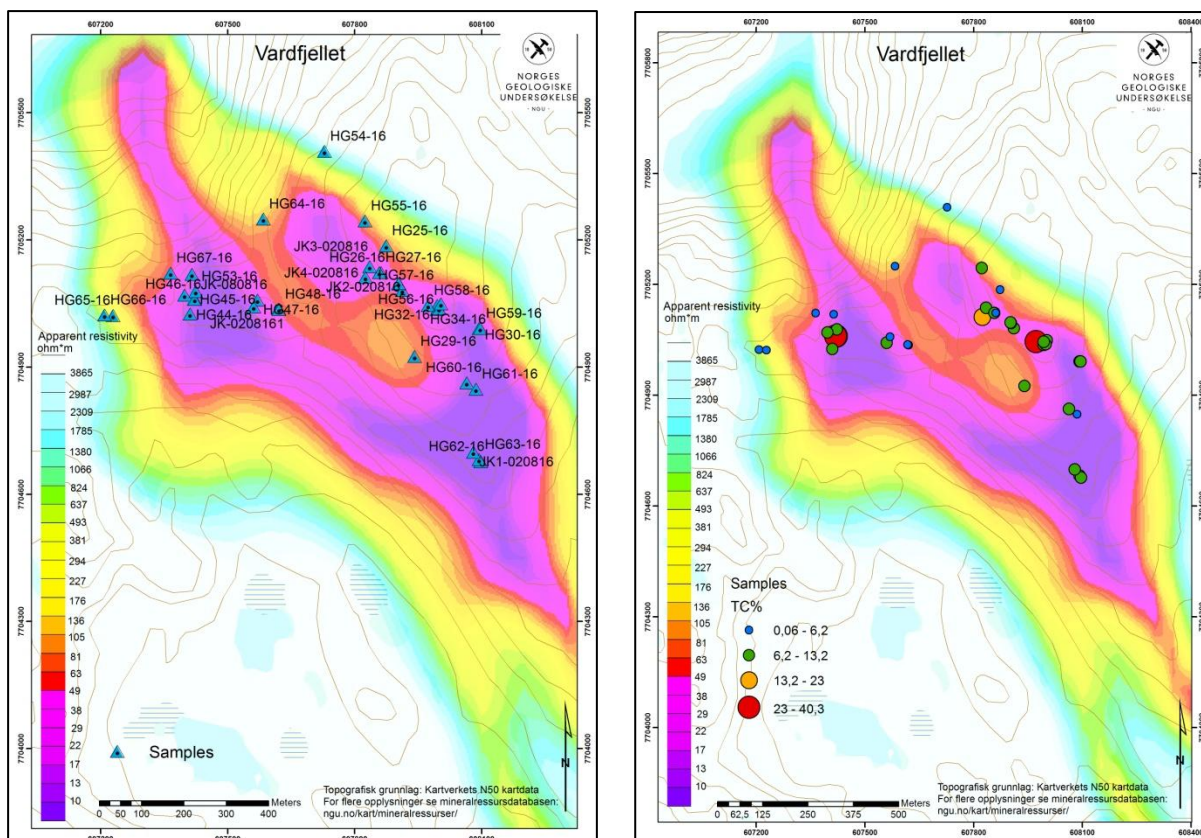


Figure 7.4: Graphite sampling points and analysed graphitic carbon content at Vardfjellet. The background is apparent resistivity calculated from frequency EM 7001 Hz (See Rodionov et al., 2013 for geophysical details).

7.3 Geological investigations at Grunnvåg

The apparent resistivity anomaly visible at the southeastern part of Lysbotn towards Grunnvåg (Figure 7.5) was unknown until the helicopter-borne geophysics was collected (Rodionov et al. 2014). The nature of this anomaly was investigated before 2016 when we found associated graphite bearings rocks along the shore of the inner part of Lysbotn. This anomaly is an obvious target for detailed ground geophysics on a later stage.

The area is almost 100 % soil covered, but graphite schist occurs in small exposures along the shoreline in the innermost part of Lysbotn. These are dissected and intruded by mafic and granitic rocks (Figure 7.6).

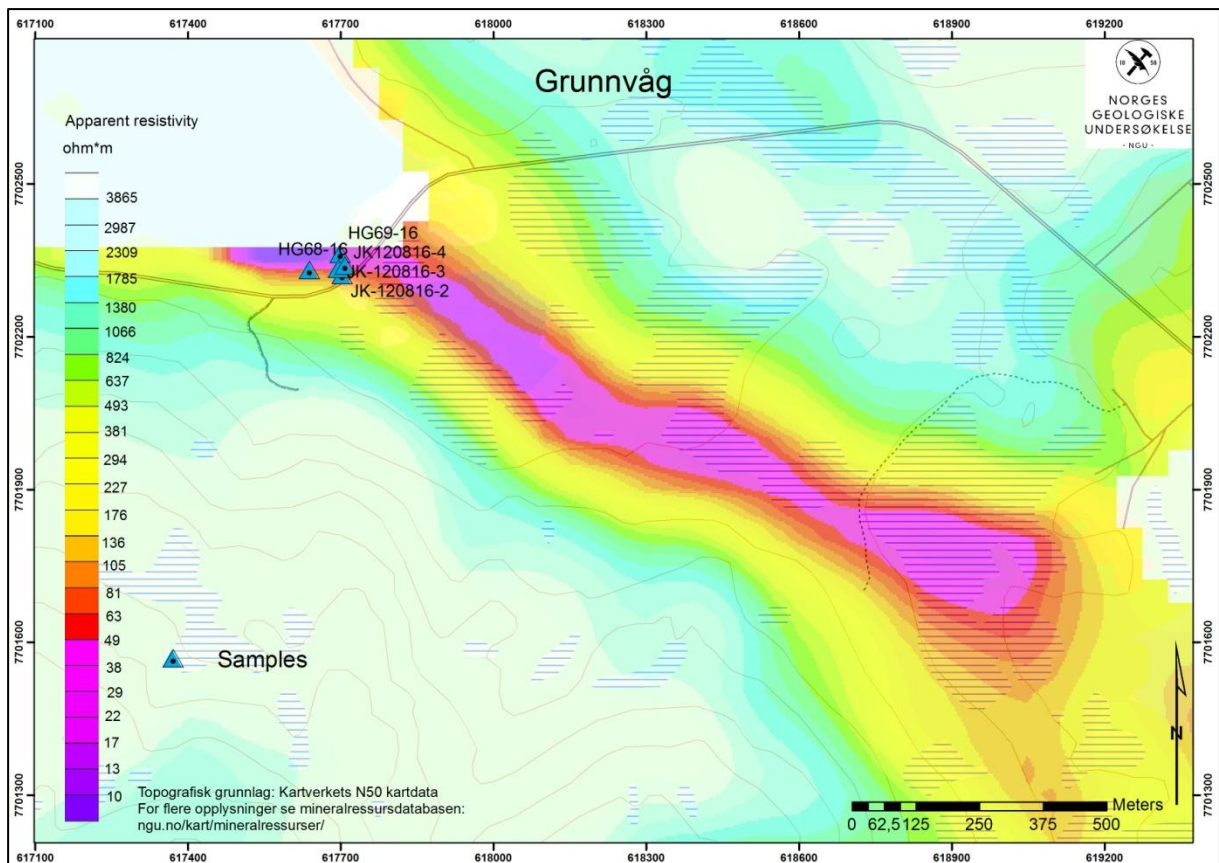


Figure 7.5: Location of sample points at Lysbotn next to Grunnvåg plotted on apparent resistivity (7001 Hz, After Rodionov et al. 2014).

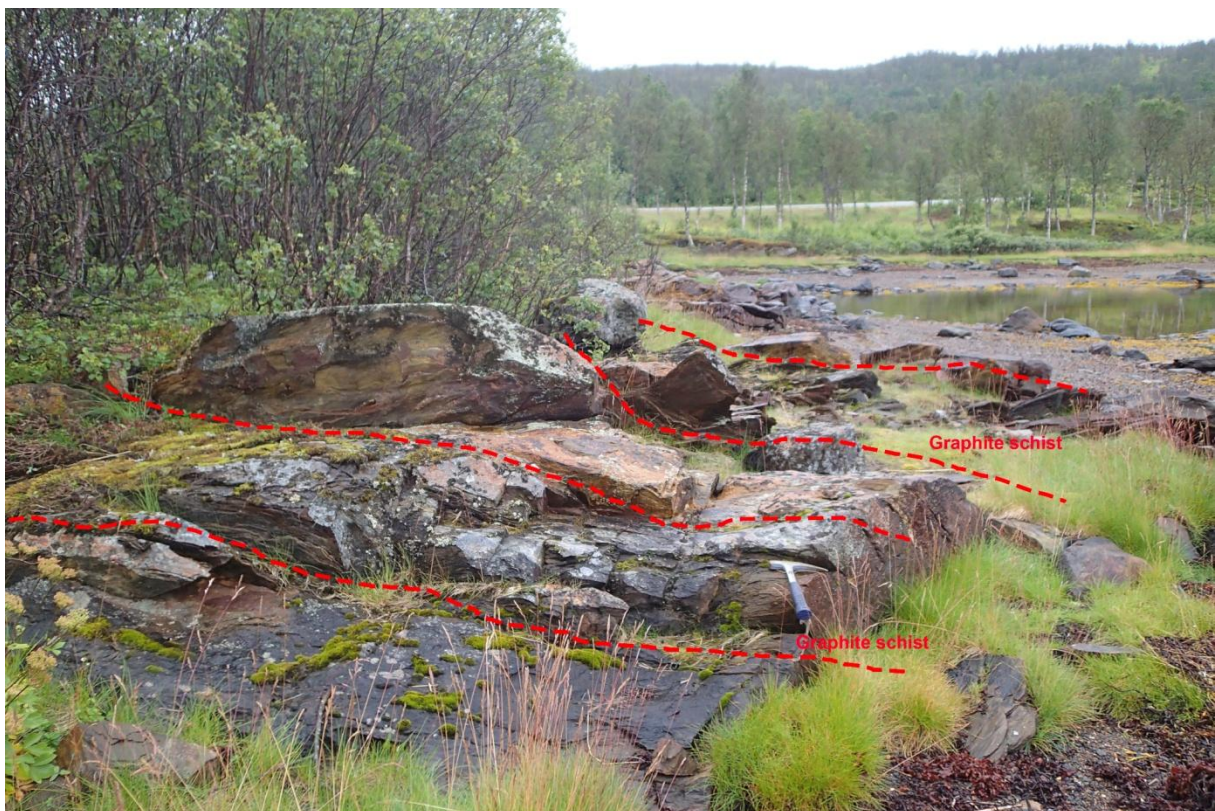


Figure 7.6: Outcrops of graphite schist cut by mafic and acid igneous rocks at the innermost part of Lysbotn (graphite bearing zones are indicated).

Five samples were collected at this locality and analysed (Table 7.1). The content of graphitic carbon varies from ca. 7 to 14.8 % Cg. This graphitic carbon content is comparable with content in deposits under development in Canada and Mozambique. The graphite schist at Grunnvåg is in part very sulphide rich. Total sulphur content varies from approximately 1% to up to 12.5 %. A sulphide content of 12.5% corresponds to a (theoretical) pyrrhotite content of approximately 34 weight %.

The Grunnvåg mineralisation should be a target for geophysical follow-up.

Table 7.1: Weight % of total sulphur (TS) and graphitic carbon (Cg) in samples from Grunnvåg.

Sample no	% TS	% Cg
HG68-16	5.00	7.41
HG69-16	<u>0.85</u>	8.46
JK-120816-2	4.58	14.85
JK-120816-3	12.50	6.72
JK120816-4	1.76	6.84

The modal content of graphite in sample JK120816-2 and JK120816-3 is given chapter 7.5.

7.4 Petrography of graphite bearing rocks

The graphite schist has a relatively simple mineralogy in thin section. The dominating minerals are quartz, feldspar (mainly orthoclase) biotite and graphite. In general there is a very limited occurrence of sulphides. An exception to the latter are the samples collected near Grunnvåg (chapter 7.3).

A typical texture of the graphite schist can be illustrated with the samples hg39-16 from Hesten, and hg45-16 from Vardfjellet (Figure 7.7 and Figure 7.8). These rocks comprise the minerals quartz, feldspar (mainly orthoclase) and biotite as the main silicate minerals. Graphite is the main opaque mineral. The quartz and feldspar show partly a granoblastic texture. The graphite crystals most commonly occur along the grain boundaries of other minerals and are often arranged parallel to other mineral particularly biotite and together they define the foliation of the rock. The crystals size of individual graphite crystals in the rock varies from approximately 50 to 2000 microns, with some samples with high carbon content where the crystal size can reach several centimetres. Figure 7.7 and Figure 7.8 covers an area of about 1.5 cm² and it is clear that in such a relatively small area the graphite can have a very uneven distribution. The same large variation over short distances as in the thin sections is observed in greater scale at the collected rock samples.



Figure 7.7: Thin section photo of graphite schist from Hesten sample Hg39-16.

The mineralogy of the graphite schist on Senja is essentially the same as in the Vesterålen area as presented by Gautneb et al., (2017) who reported results from bench scale beneficiation tests of Vesterålen graphite schists. The tests were successful, and by standard methods it is possible to obtain a final graphite concentrate with more than 95 % graphite carbon with good recovery (See Gautneb et al. 2017 for details). In all likelihood, such results will also be possible with rocks from Vardfjellet and Hesten.

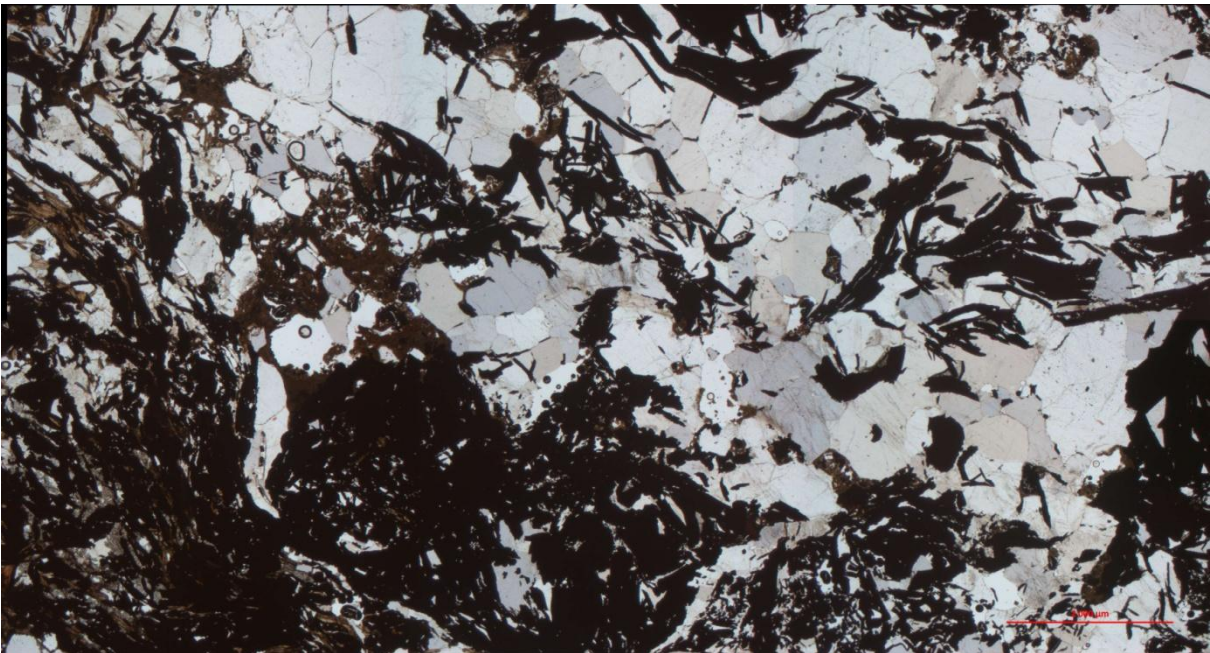


Figure 7.8: Thin section photo of graphite schist from Vardfjellet sample Hg45-16

7.5 Modal content of graphite

When thin sections are made it is interesting to measure the modal content of graphite (volume %) in selected rocks, using the methods described in chapter 4.2. Table 7.2 show the results of the measurements of modal graphite. This was done on a few selected thin sections to get an impression of which content of modal graphite are present.

Table 7.2: Modal % of graphite and weight percent of graphitic carbon (Cg) in some selected samples from Hesten, Vardfjellet, Bukkemoen and Grunnvåg.

Sample	Locality	Vol % graphite	% Cg
hg39-16	Hesten	22.2	12.8
hg24-14	Hesten	12.6	4,0
hg30-14	Hesten	4.6	5.5
jk4-020816	Vardfjellet	21.2	6.7
hg45-16	Vardfjellet	30.9	23.6
jk110816-1	Bukkemoen	6.1	5.1
JK120816-2	Grunnvåg	26.8	14.9
JK120816-3	Grunnvåg	34.8	6.7

Some samples were also included from Bukkemoen and Grunnvåg. Other things being equal the modal or volume % of graphite will always be larger than the weight % (% Cg) in a rock. However this relationship is never straight forward since a thin section only represent about 3 cm² and a chemical analysis represents a hand size (or larger) sample. Sample heterogeneity will strongly affect the modal measurements of graphite.

The three samples from Hesten show a variation of modal graphite content from 4.6 to 22.2 % and the two samples from Vardfjellet show a content of 22.2% and 30.9 % respectively.

7.6 Summary of sulphide and carbon analysis

A total of 63 surface samples of graphite schist were collected at different outcrops along the geophysical anomaly that defines the graphite mineralised areas (Figures 7.1, 7.4 and 7.5). Care was taken to get as representative a sample collection as possible. A table of all individual analysis is given in Appendix 1. The data is summarised in Table 7.3 and in Figure 7.9.

Table 7.3: Summary of graphitic carbon content in samples from Hesten, Vardfjellet and Grunnvåg.

Locality	N	Average (Cg)	Max (Cg)	Min(Cg)	Stdv.
Vardfjellet-Hesten-Grunnvåg (aggregated)	63	8.0	40.3	1.1	6.2
Hesten	21	5.8	12.81	1.72	3.02
Vardfjellet	37	9.2	40.30	1.12	7.49
Grunnvåg	5	8.9	14.85	6.72	3.42

There is a very large variation in the composition of the graphite schist with regards to content of graphitic carbon, with a difference of almost 40 % between the maximum and minimum samples. The median value of graphitic carbon for all samples at Vardfjellet and Hesten is 7.7 % Cg.

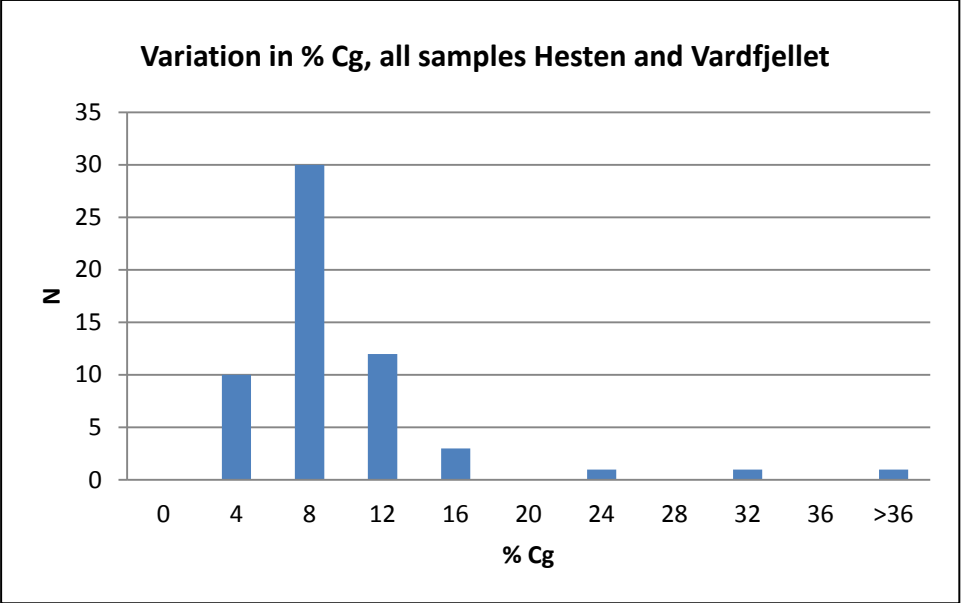


Figure 7.9: Histogram showing the spread in % Cg for all samples collected at Hesten and Vardfjellet.

On average Vardfjellet has a 3.5% higher content of graphitic carbon than Hesten. Hesten has a somewhat more uniform graphitic carbon content with a lower standard deviation. It is believed that these results give as good as possible measurement of the content of graphitic carbon in these deposits. Systematic drilling is necessary to give a more precise estimate.

The spatial distribution of our sample points and variation in graphite grade are shown on Figure 7.2 and 7.5. There is no apparent systematic variation and over short distances perpendicular and along strike of individual graphite lenses, the content of graphitic carbon can vary with more than 10%. We believe that including the outliers (both high and low %Cg) among the samples will give a more realistic average composition that will approach what could be expected in a mining situation.

8. 3D PHOTOGRAMMETRY AND GEOLOGICAL MODELLING

In this chapter 3D models from Hesten and Vardfjellet are presented. The two 3D models were created with the programs Agisoft Photoscan Professional and 3D-MOVE as described in the methodology above. These models can be delivered in a digital version in 3D PDF format from NGU on request to researcher Iain Henderson.

8.1 3D drone photogrammetry modelling at Hesten

According to the photogrammetric method detailed described above in Chapter 4.3, we have constructed a 3D model of the Hesten graphite deposit. This was based on the original surface geological mapping carried out by Henderson & Kendrick (2003) and the geophysical and photogrammetric surveys carried out here. Figure 8.1 shows the elevation model newly imported into the 3D MOVE software without any added geology. Figure 8.2 shows the same view with the drone topography made transparent such that the geology is apparent. Here we see the NW-SE trending greenstone rocks (green) below and enveloping the graphite on the Hesten ridge. The meta-supracrustals are isoclinally folded on N-S axes. The graphite (blue) forms two NW-SE ridge-parallel zones dipping steeply NW in the east and steeply SE in the west. The northern limit of the deposit is truncated by an E-W trending fault (red).

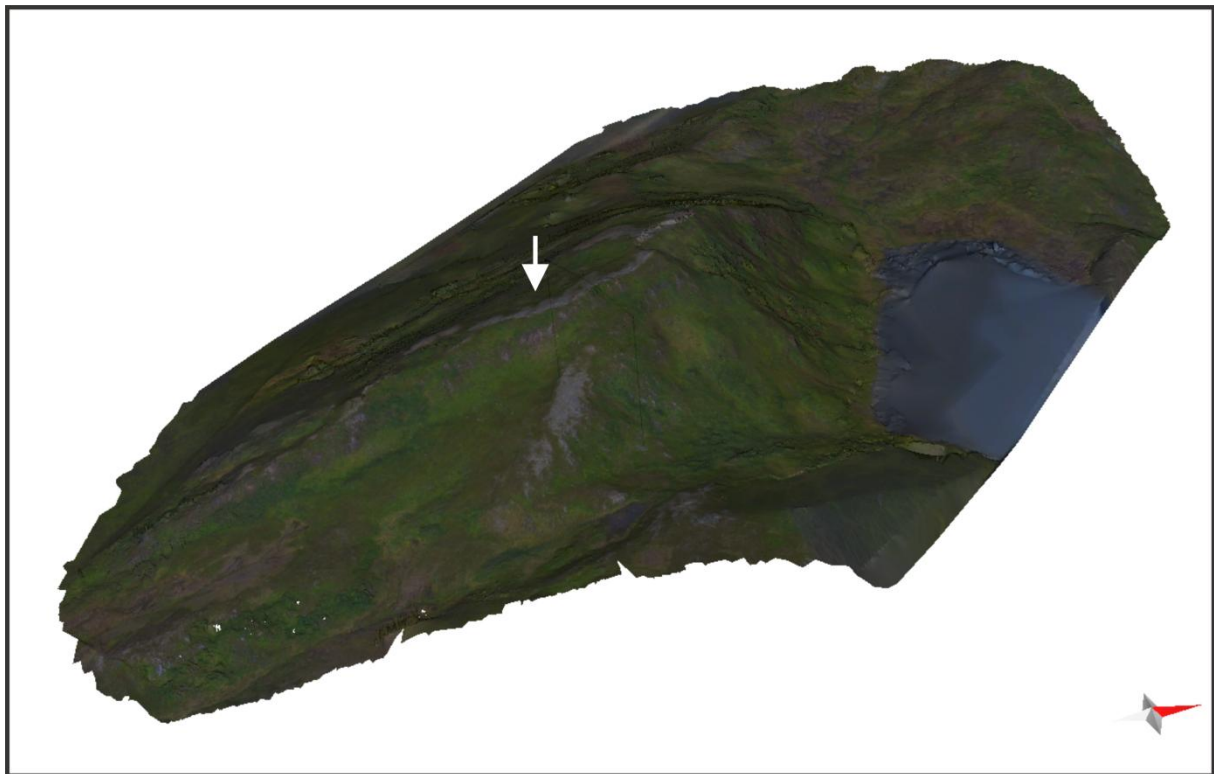


Figure 8.1: View of the Hesten deposit seen from the south east, showing the elevation model with the orthophotos draped over the elevation model. The white arrow shows the trend of a series of outcrops which is observed as a grey/brown colour in the model and is the linearly outcropping graphite

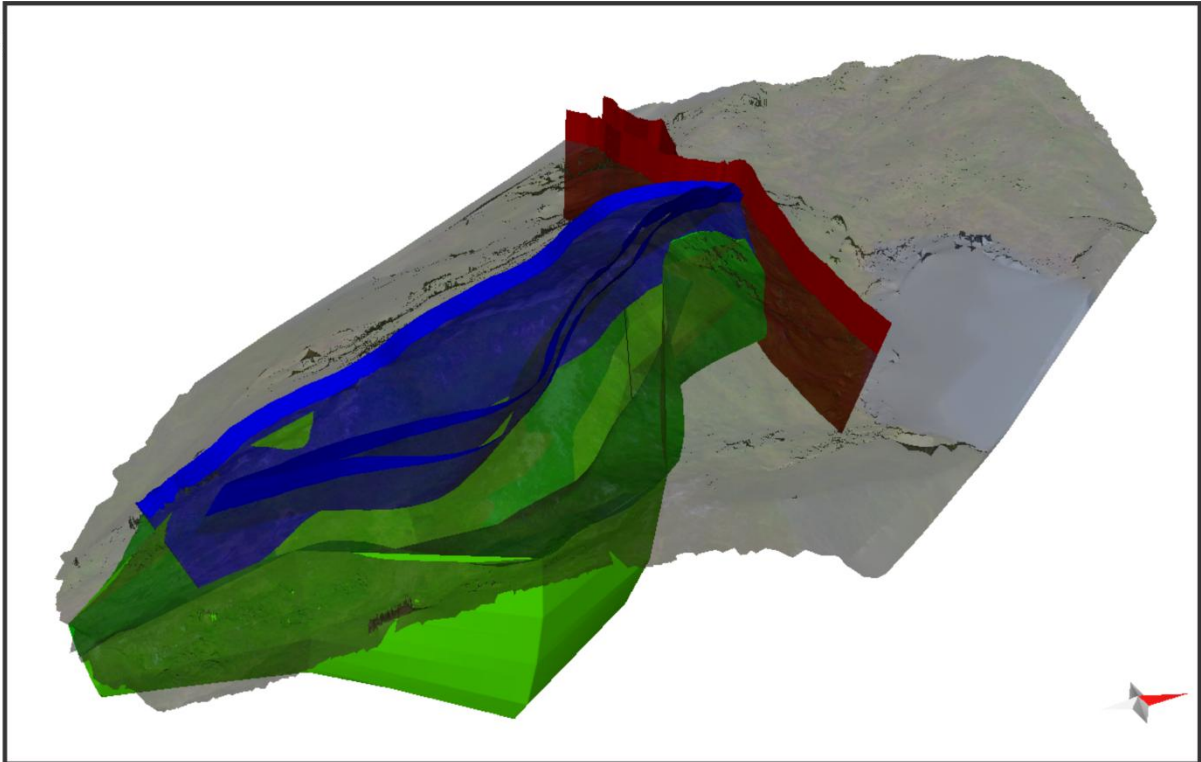


Figure 8.2: View of the Hesten deposit seen from the south east, showing the elevation model with the orthophotos draped over the elevation model. The elevation model is made transparent such that the geology is visible. The enveloping meta-supracrustals are seen in green and the graphite layers in blue. The northern margin of the deposit (right) is truncated by an east west fault.

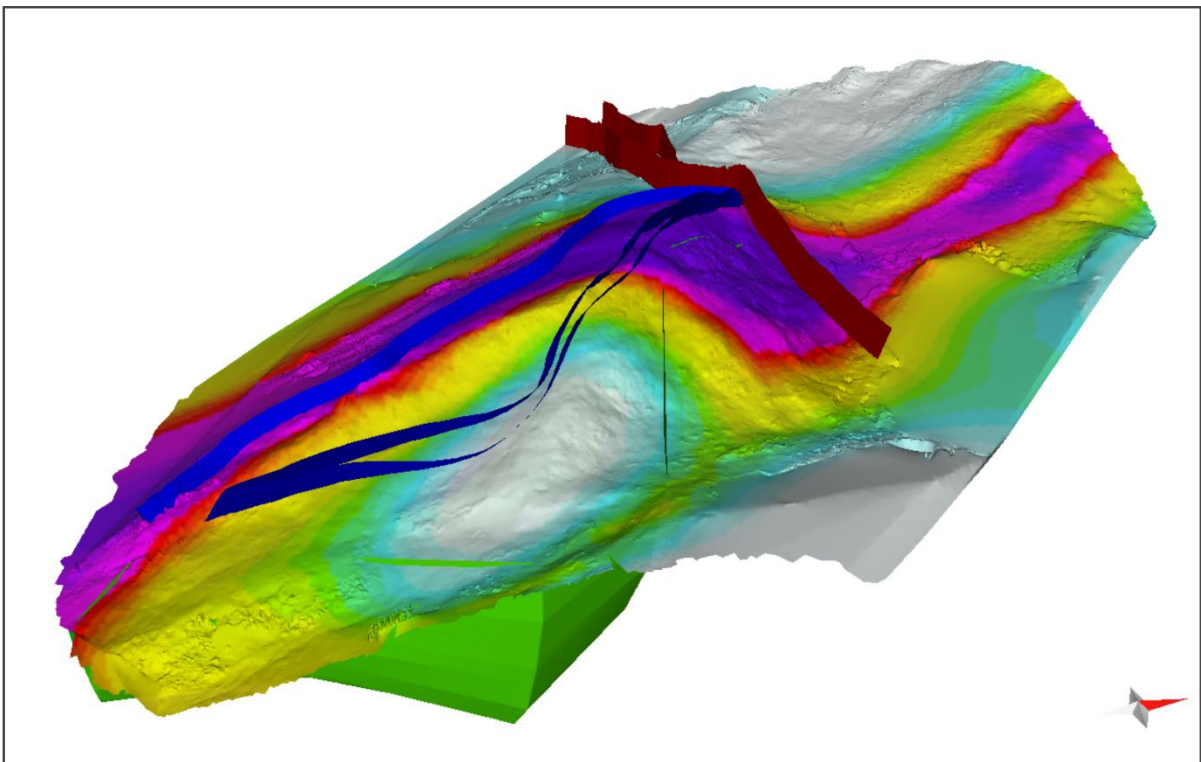


Figure 8.3: View of the Hesten deposit seen from the east, showing the EM anomaly map over the elevation model. The elevation model is made transparent such that the geology is visible. The enveloping amphibolitic schists are green and the graphite layers are blue. An E-W trending fault is shown in brown. The EM anomaly coincides with the general exposure of the folded graphite layers.

Figure 8.3 shows the same view with the EM anomaly and shows more clearly the two linear graphite layers. The EM anomaly clearly coincides with the Hesten ridge and the mapped graphite at the surface. The EM anomaly becomes markedly thinner to the north of the E-W fault.

8.2 3D drone photogrammetry modelling at Vardfjellet

According to the photogrammetric method detailed described in chapter 4.3, we have constructed a 3D model of the Vardfjellet graphite deposit. This was based on the original surface geological mapping carried out by Henderson & Kendrick (2003) and the geophysical and photogrammetric surveys carried out here. Figure 8.4 shows the elevation model newly imported into the 3D MOVE software. Figure 8.5 shows the same view with the drone topography made transparent such that the geology is apparent. Here we see the NW-SE trending greenstone rocks (green) folded in rather tight folds with N-S axes. The graphite (blue) is segmented and forms generally isolated isoclinal geometries. In the northern part of the deposit, the greenstone F_2 fold axes are re-folded along F_3 open fold axes. This northern part of the deposit is intensely segmented by N-S striking F_3 shear zone and faults (Figure 8.6) and here there are many separate occurrences of graphite.

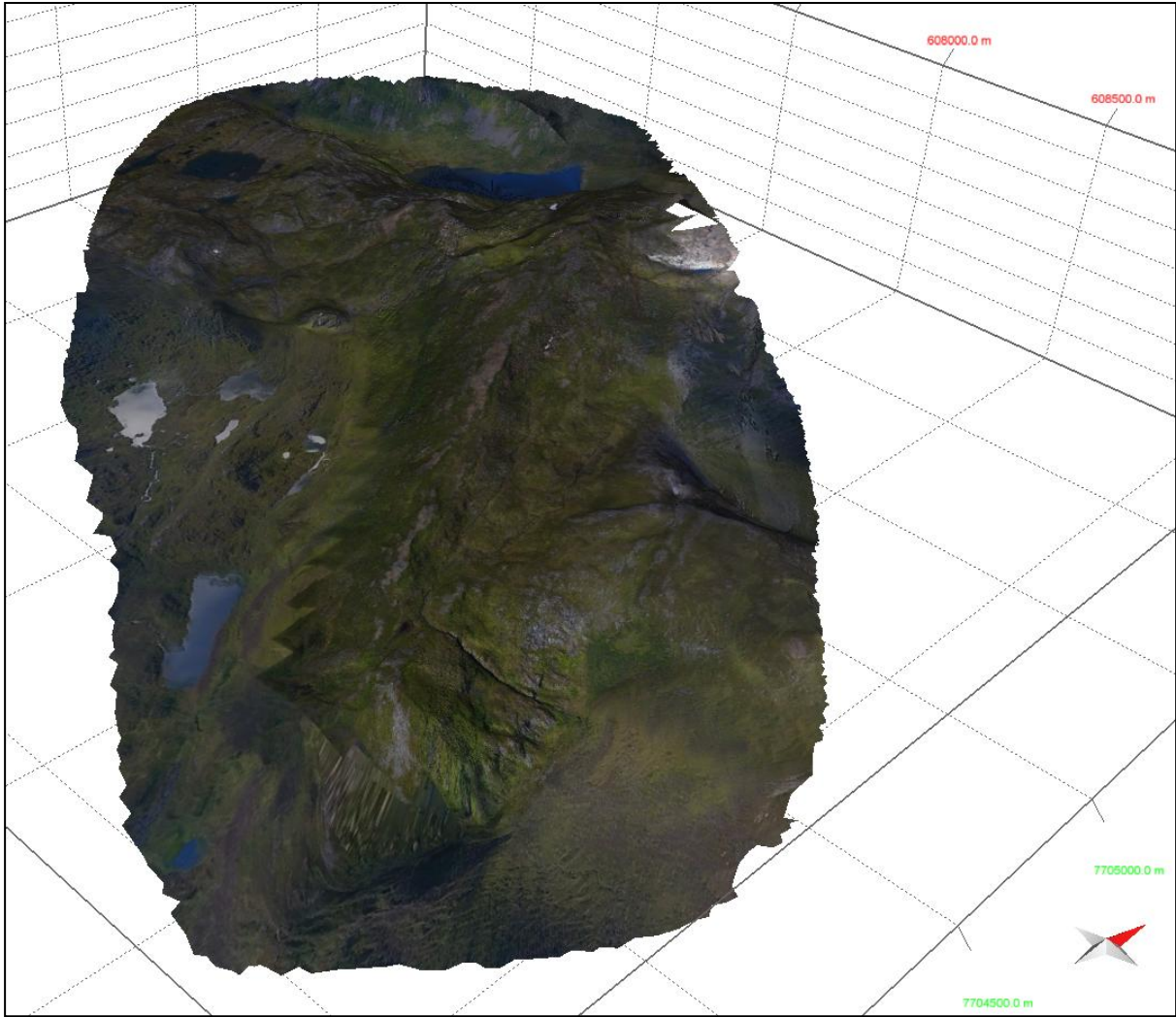


Figure 8.4: View of the Vardfjellet deposit seen from the south east, showing the elevation model with the orthophotos draped over the elevation model.

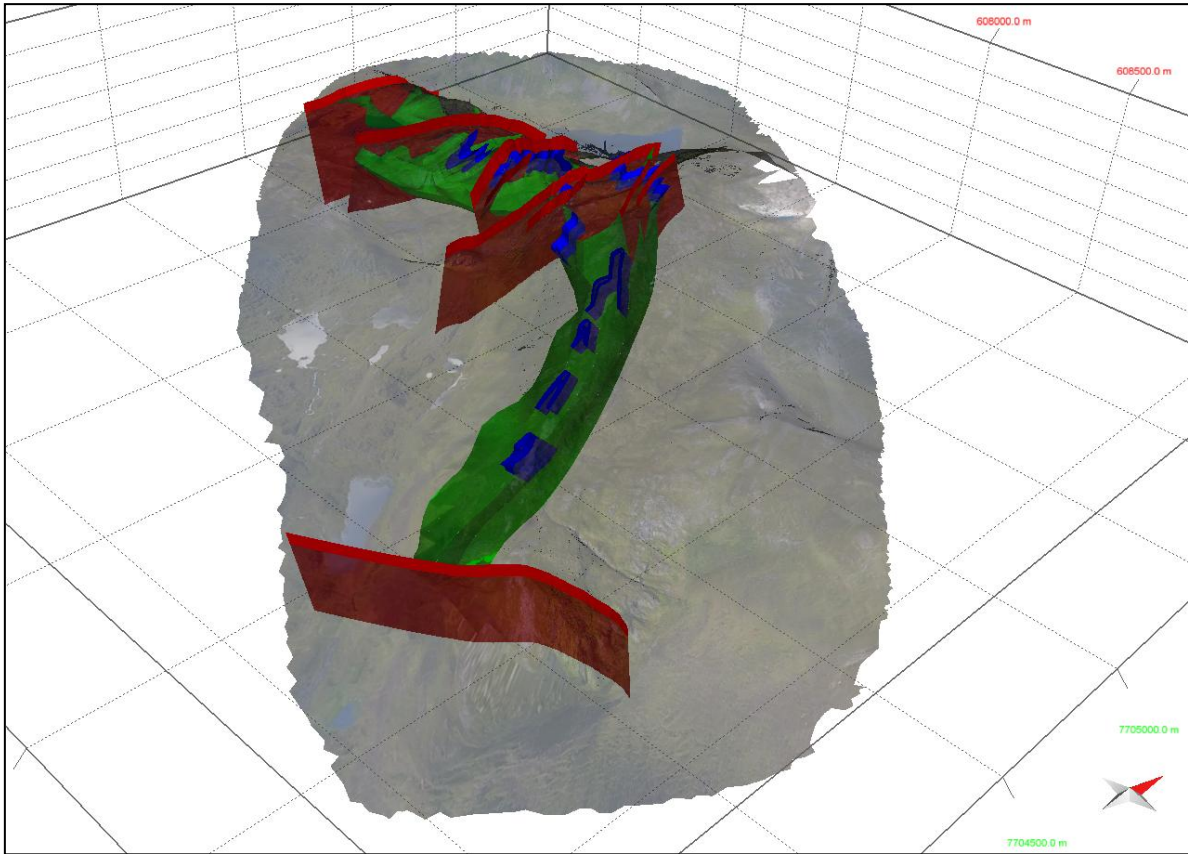


Figure 8.5: View of the Vardfjellet deposit seen from the south east, showing the elevation model with the orthophotos draped over the elevation model. The elevation model is made transparent such that the geology is visible.

Figure 8.7 shows the relationship between the regional EM anomaly and the outcropping graphite and metasediments surrounded by the granitic gneisses. There is a clear coincidence of the graphite and the EM anomalies. The EM anomalies also appear to be affected by the WNW-ESE faults. For example, at the southern part of the deposit, the EM anomaly appears truncated and thins out directly SE of the fault (Figure 8.7). In addition, in the NW part of the deposit, where the graphite is terminated in the F_3 folded F_2 fold hinge, the anomaly truncation is coincident with the mapped graphite outcrop termination.

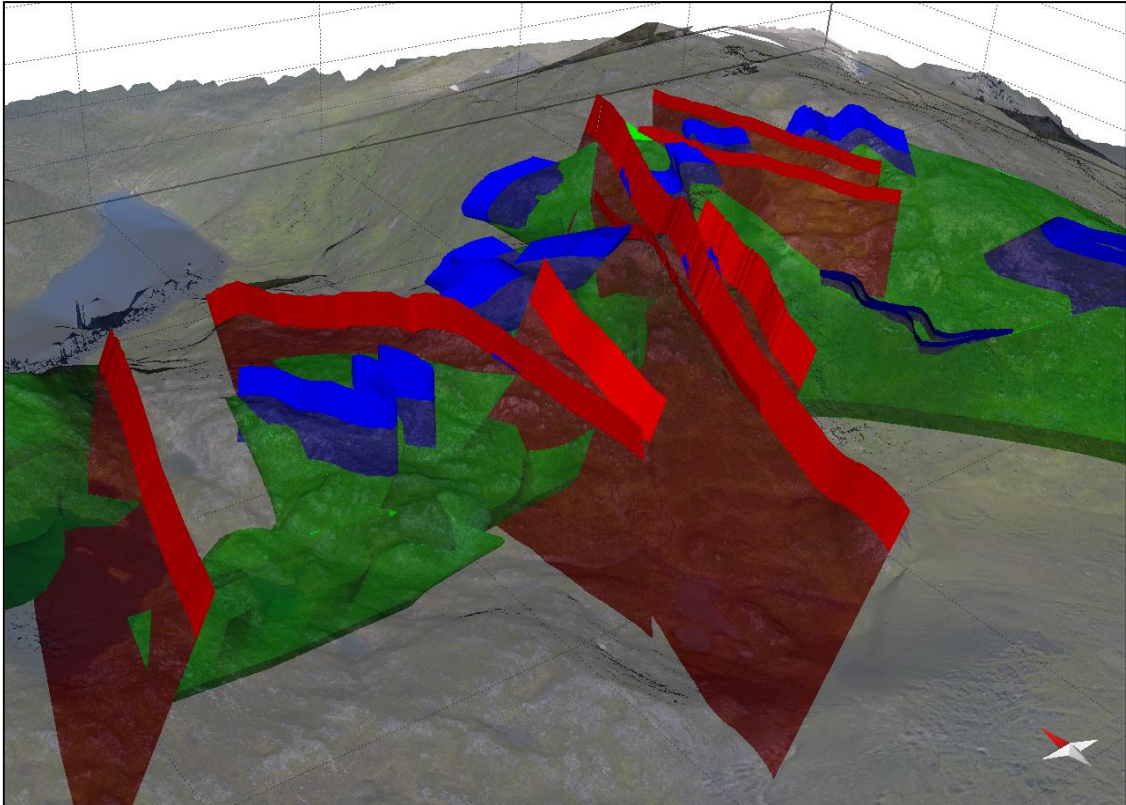


Figure 8.6: The northern part of the Vardfjellet deposit showing the complexly folded graphite (blue) and the enveloping greenstone rocks (green). In this part of the deposit, the generally N-S F2 fold axes of the greenstones are deformed around open F3 fold hinges such that the F2 fold hinges are E-W. The F3 fold hinge is complexly dissected by F3 faults and shear zones (red).

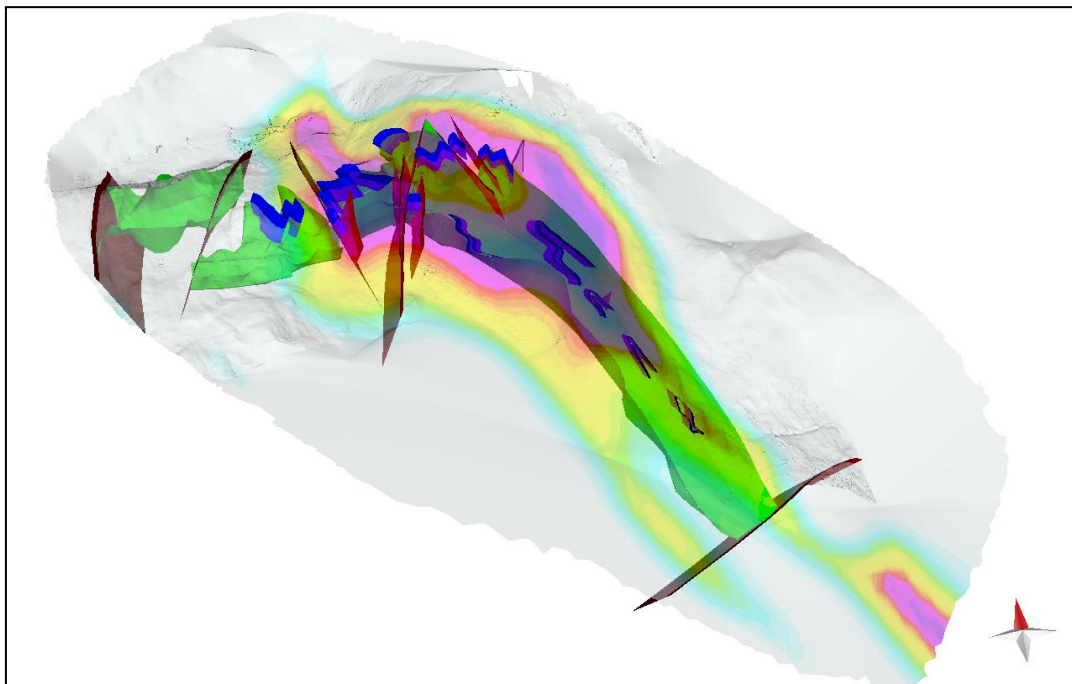


Figure 8.7: View of the Vardfjellet deposit seen from the east, showing the EM anomaly map over the elevation model. The elevation model is made transparent such that the geology is visible. The enveloping amphibolitic schists are green and the graphite layers are blue. The EM anomaly coincides with the general exposure of the complexly folded graphite layers.

9. SUMMARY AND CONCLUSIONS

At Hesten and Vardfjellet geophysical and geological follow-up work has been performed. At Grunnvåg, only some sampling, analysis and thin section studies were undertaken.

9.1 Summary and conclusions, Hesten

At **Hesten**, outcropping graphite mineralisations are mapped in a length of ca. 1 km. The graphite is partly soil covered, and geophysical mapping indicates graphite in a total length of ca. 2 km. The total width of the mineralised zone is from ca. 100 up to ca. 400 m. There is strong evidence that there are several graphite zones, possibly up to 8 – 10 individual zones. The thickness of these is measured to 3 – 4 meters at two locations. However, we have no data for all the individual zones, and the actual thickness could be more. The outcropping graphite layer dips steeply (ca. 70 °) to the west at the surface. Charged Potential measurements (CP) indicates that graphite bodies are electrically connected, and the size (length along strike and depth extend) of individual lenses is not possible to map using the CP method.

The graphite appears partly enriched in individual layers and partly evenly distributed in the rock. The dominating minerals are quartz, feldspar (mainly orthoclase), biotite and graphite. In general there is a very limited sulphide occurrence. The individual graphite crystals size in the rock varies from approximately 50 to 2000 microns. Some samples have high carbon content where the crystal size can reach several centimetres. The mineralisations appear as flake graphite.

In total 21 samples from the Hesten area were analyzed for graphitic carbon (Cg) and total sulphur content. Individual sampling points and analysis are presented. The average Cg content is 5.8 % with a maximum and minimum of 12.8 % and 1.7 %. The standard deviation is 7.5 %. The average sulphur content in samples from Hesten is 0.2 % with a maximum value of 0.9 %.

Bedrock and structural investigations have previously been performed by Henderson & Kendrick (2003) and shows that the graphite schist on the surface consists of several apparently isolated lenses that are isoclinally folded and refolded. Complex structural episodes have both created and modified the graphite deposits and the graphite is intimately associated with the development of F2 folds, as graphite is best developed geographically in association with north-south striking F₂ fold hinges. In addition to the folding, several deformation sequences have influenced the graphite structures. To get a better control on the 3D structures, drone based photogrammetry and geological modeling were performed and presented in this project. A 3D structural model in pdf format is available from NGU on request.

Despite the relatively low graphitic content in the Hesten mineralisation (average 5.8 %), the total area of graphite is quite large and the potential for economic mineralisation is high. This graphitic carbon content is comparable with content in deposits under development in Canada and Mozambique. NGU recommends further investigation with detailed ground electromagnetic measurements prior to core drilling. This activity is outside of the scope of studies for NGU and must be financed by a prospecting company.

9.2 Summary and conclusions, Vardfjellet.

At **Vardfjellet**, the graphite mineralisations are more exposed than at Hesten, and graphite can be found exposed over an area of 1.7 km in length and up to 350 metres in width. Geophysical mapping indicates graphite in a total length of ca. 2 km. The total width of the mineralised zone is from ca. 100 up to ca. 480 m. There is strong evidence that there are several zones, possibly up to 6 – 8 individual zones. The individual thickness of these is observed to be 7 m at one location and measured to 3 – 5 meters at two other locations. However, we have no data for all of the individual zones, and the thickness could be more. Due to the intense folding observed at Vardfjellet, the dip of the graphite zones varies but dips mostly steeply towards the west. Charged Potential measurements (CP) indicates that the graphite bodies are electrically connected, and the size (length along strike and depth extend) of individual lenses is not possible to map using the CP method.

The graphite appears partly enriched in individual layers and partly evenly distributed in the rock. The dominating minerals are quartz, feldspar (mainly orthoclase), biotite and graphite. In general there is limited sulphide occurrence. The individual graphite crystals size in the rock varies from approximately 50 to 2000 microns, with some samples with high carbon content where the crystal size can reach several centimetres. The mineralisations appear as flake graphite.

In total 37 samples from the Vardfjellet area were analyzed for graphitic carbon (Cg) and total sulphur content. Individual sampling points and analyses are presented. The average Cg content is 9.2 % with a maximum and minimum of 40.3 % and 1.1 %. The standard deviation is 7.5 %. Total sulphur content at Vardfjellet is slightly higher than at Hesten, with an average of 0.3 % with a maximum value of 1.3 %.

As for Hesten, bedrock and structural investigations have previously been performed by Henderson & Kendrick (2003) and shows that the graphite schist on the surface consists of several apparently isolated lenses that are isoclinally folded and refolded. Complex structural events have both created and modified the graphite deposits and the graphite is intimately associated with the development of F2 folds, as graphite is best developed geographically in association with north-south striking F2 fold hinges. In addition to the folding, several deformation episodes have influenced the graphite structures. To obtain a better control on the 3D structures, drone based photogrammetry and geological modeling were performed in this project. A 3D structural model in pdf format is available from NGU on request.

Despite the relatively low graphitic content in the Vardfjellet mineralisation (average 9.2 %), the total area of graphite is quite large, and the potential for economic mineralisations is high. This graphitic carbon content is comparable with content in deposits under development in Canada and Mozambique. To get a better understanding of how high grade graphite occurs at Vardfjellet, NGU recommends further investigation with ground electromagnetic measurements prior to core drilling. This activity is outside of the scope of studies by NGU and must to be financed by a prospecting company.

9.3 Summary and conclusions, Grunnvåg

At Grunnvåg, a ca. 1.5 km long and ca.100 m wide apparent resistivity anomaly from helicopter-borne electromagnetic measurements was observed. Originally this was thought to be caused by seawater intrusions into the sediments but field investigations revealed a new graphite mineralisation. No geophysical follow-up work was performed at Grunnvåg.

The area is almost 100% soil covered, but graphite schist occurs in small exposures along the shoreline in the innermost part of Lysbotn. These are dissected and intruded by mafic and granitic rocks.

From one exposure in the Grunnvåg area 5 samples were analyzed for graphitic carbon (Cg) and total sulphur content. Individual sampling points and analysis are presented. The average Cg content is 8.9 % with a maximum and minimum of 14.8 % and 6.7 %. The standard deviation is 3.4 %. Total sulphur content at Grunnvåg is much higher than at Hesten and Vardfjellet and varies from about 1 to up to 12.50 %. A sulphide content of 12.5% corresponds to a (theoretical) pyrrhotite content of about 34 weight %.

The Grunnvåg anomaly is a target for detailed ground geophysics at a later stage.

9.4 Beneficiation test

The mineralogy of the graphite schist on Senja is essentially the same as in the Vesterålen area. Gautneb (et al. 2017) reported results from bench scale beneficiation tests of Vesterålen graphite schists. The results were successful, and by standard methods it is possible to obtain a final graphite concentrate with more than 95% graphite carbon and a good recovery (See Gautneb et al. 2017 for details). In all likelihood, such results will also be possible with rocks from Vardfjellet and Hesten.

10. REFERENCES

- AarhusInv, 2013. *Manual for Inversion software ver 6.1*, Aarhus, Denmark: Hydro Geophysics Group (HGG), University of Aarhus.
http://www.hgg.geo.au.dk/HGGsoftware/em1dinv/em1dinv_manual.pdf .
- ABEM, 2012. *ABEM Terrameter LS. Instruction Manual, release 1.11*, Sundbyberg: ABEM Instrument AB, Sweden.
- Dahlin, T., 1993. *On the automation of 2D resistivity surveying for engineering and environmental applications..* Lund: Department of Engineering Geology, Lund Institute of Technology, Lund University. 187pp, ISBN 91-628-1032-4.
- Dahlin, T. & Zhou, B., 2006. Multiple-gradient array measurements for multichannel 2D. *Near Surface Geophysics, Vol 4, No 2*, April, pp. 113-123.
- Dalsegg E. 1985: Geofysiske bakkemålinger Krokeldalen og Geitskaret, Senja Troms NGU report 85.188
- Dalsegg, E. 1986: Elektriske målinger i Skalands gruveområde, Senja, Troms. NGU Rapport 86.179.
- Dalsegg, E., 1994. *CP-, SP- og ledningsevne målinger ved grafittundersøkelser ved Hornvannet, Sortland, Nordland*, Trondheim: NGU Report 94.003.
- Gautneb, H., Knezevic, J., Johannesen, N.E., Wanvik, J.E., Engvik, A., Davidsen, B., Rønning, J.S. 2017: Geological and ore dressing investigations of graphite occurrences in Bø, Sortland, Hadsel and Øksnes municipalities, Vesterålen, Nordland County, Northern Norway 2015 – 2016. NGU Report 2017.015 (70pp.).
- Geosoft, 1997. *HEM System (Helicopter Electromagnetic data Processing, Analysis and Presentation System*, Toronto, Ontario Canada: Geosoft.
- Geotech, 1997. *Hummingbird Electromagnetic System, User manual*, s.l.: Geotech Ltd.
- Heldal & Lund 1987: Bergrunnsgeologisk kartlegging i Berg kommune Senja (1:5000). unpublished NGU map.
- Henderson, I.H.C., Kendrick, M. 2003: Structural controls on graphite mineralisations, Senja, Troms -2003, NGU report 2003.011.
- Keilhau 1844: Beretning om en geonostisk reise i norlandene i 1855. *Nyt Magazin for naturvidenskaberne*. 11, nr.3
- Kihle, O. & Eidsvig, P. D., 1978. *Nye tolkninger for tolkning av CP-målinger*, Trondheim: NGU.
- Lauritsen T. 1988: CP-,SP og VLF målinger bukkemoen, Senja- 1988. NGU report 86.186
- Loke, M. H., 2014. *Geoelectrical Imaging 2D & 3D. Instruction Manual. Res2DInv ver 4.00*. <http://www.geotomosoft.com/>.
- Myhre, P.I., Corfu, F., Bergh, S.G. & Kullerud, K. 2013: U-Pb geochronology along an Archean geotranssect in the West-Troms Basement complex, North Norway. *Norwegian journal of Geology*, 93,1-24.
- Rodionov, A., Ofstad, F., Stampolidis, A., Tassis, G. 2014: Helicopter-borne magnetic, electromagnetic and radiometric geophysical survey 2012, 2013 and 2014, Troms County. NGU report 2014.039
- Rønning, J.S., Rodionov, a., Ofstad, F., Lynum R. 2012: Elektromagnetiske, magnetiske, og radiometriske målinger fra helikopter i området Skalands - Trælen på Senja. NGU report 2012.061.

- Rønning, J. S. et al., 2014. Oppfølgende grafittundersøkelser i Meløy og Rødøy kommuner, Nordland, Trondheim: NGU. Report nr 2014.046.
- Rønning, J. S., Rodionov, A., Ofstad, F. & Lylum, R., 2012. Elektromagnetiske, magnetiske og radiometriske målinger fra helikopter i området Skaland - Trælen på Senja, Trondheim: NGU Report 2012.061.
- Sato, M. & Mooney, H. M., 1960. The electrochemical mechanism of sulfide self-potentials. *Geophysics*, Volume 25, pp. 226-249.
- UBC, 2000. Manual for EM1DFM., Vancouver, Canada: UBC - Geophysical Inversion facility, Department of Earth and Ocean Sciences, University of British Columbia.
- Zwaan, K.B., Fareth, E. 2005: Bergrunnsgeologisk kart Melfjordbotn 1433 IV, 1:50000. Norges geologiske undersøkelse.

APPENDIX 1, 2 and 3 follows.

Appendix 1: Analyses of total sulphur (TS) and graphic (Cg) carbon from Vardfjellet, Hesten and Grunnvåg. (UTM zone 33N).

NGU_no	Year	Locality	Easting	Northing	Sampler	Sample no	Text	% TS	% Cg
137101	2016	Vardfjellet	607873	7705186	Håvard Gautneb	HG25-16	Medium grade graphite schist	0.35	5.22
137102	2016	Vardfjellet	607861	7705123	Håvard Gautneb	HG26-16	Medium grade graphite schist	0.41	4.77
137103	2016	Vardfjellet	607857	7705123	Håvard Gautneb	HG27-16	Medium grade graphite schist	0.38	6.86
137104	2016	Vardfjellet	607618	7705037	Håvard Gautneb	HG28-16	Medium grade graphite schist	0.47	5.57
137105	2016	Vardfjellet	607940	7704925	Håvard Gautneb	HG29-16	Medium grade graphite schist	0.58	9.11
137106	2016	Vardfjellet	608092	7704991	Håvard Gautneb	HG30-16	Rich graphite schist	0.30	10.38
137107	2016	Vardfjellet	607993	7705045	Håvard Gautneb	HG31-16	Weathered rusty low grade graphite schist	0.03	6.77
137108	2016	Vardfjellet	607993	7705036	Håvard Gautneb	HG32-16	Weathered rusty low grade graphite schist	0.12	8.36
137109	2016	Vardfjellet	607998	7705038	Håvard Gautneb	HG33-16	Medium grade and strongly weathered graphite schist	0.02	7.70
137110	2016	Vardfjellet	608002	7705049	Håvard Gautneb	HG34-16	Medium grade and strongly weathered graphite schist	0.21	12.60
137119	2016	Vardfjellet	607397	7705070	Håvard Gautneb	HG43-16	Low grade graphite schist	0.26	7.07
137120	2016	Vardfjellet	607410	7705025	Håvard Gautneb	HG44-16	Very rich graphite schist	0.36	7.08
137121	2016	Vardfjellet	607419	7705060	Håvard Gautneb	HG45-16	Very rich graphite schist	0.14	23.60
137122	2016	Vardfjellet	607421	7705060	Håvard Gautneb	HG46-16	Very rich graphite schist	0.06	40.30
137123	2016	Vardfjellet	607569	7705058	Håvard Gautneb	HG47-16	Medium grade graphite schist	0.14	6.12
137124	2016	Vardfjellet	607620	7705036	Håvard Gautneb	HG48-16	Medium grade graphite schist	0.30	5.76
137129	2016	Vardfjellet	607423	7705078	Håvard Gautneb	HG53-16	Medium grade graphite schist	0.66	9.54
137130	2016	Vardfjellet	607727	7705409	Håvard Gautneb	HG54-16	Very rich graphite schist	0.34	5.48
137131	2016	Vardfjellet	607823	7705245	Håvard Gautneb	HG55-16	Medium grade graphite schist	0.03	6.53
137132	2016	Vardfjellet	607903	7705096	Håvard Gautneb	HG56-16	Good quality graphite schist	0.13	9.98
137133	2016	Vardfjellet	607911	7705081	Håvard Gautneb	HG57-16	Good quality graphite schist	0.17	10.98
137134	2016	Vardfjellet	607972	7705045	Håvard Gautneb	HG58-16	Good quality graphite schist	0.02	31.35
137135	2016	Vardfjellet	608095	7704991	Håvard Gautneb	HG59-16	Medium grade graphite schist	0.48	9.48
137136	2016	Vardfjellet	608063	7704863	Håvard Gautneb	HG60-16	Medium grade graphite schist	0.12	9.48
137137	2016	Vardfjellet	608085	7704848	Håvard Gautneb	HG61-16	Medium grade graphite schist	0.42	5.34

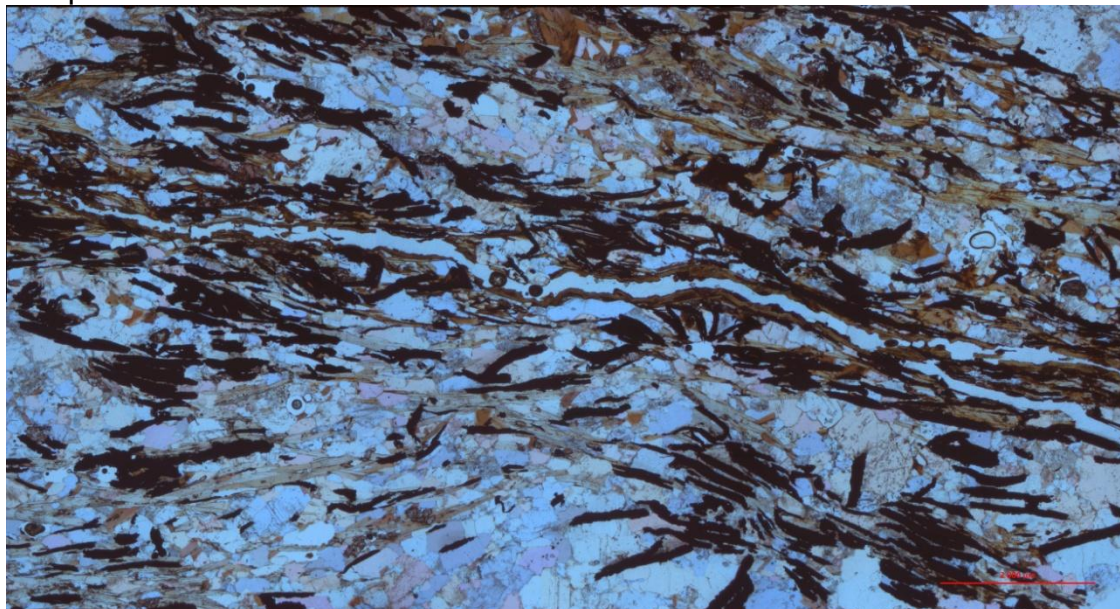
137138	2016	Vardfjellet	608096	7704677	Håvard Gautneb	HG62-16	Medium grade graphite schist	0.22	6.50
137139	2016	Vardfjellet	608092	7704682	Håvard Gautneb	HG63-16	Medium grade graphite schist	0.34	6.56
137140	2016	Vardfjellet	607583	7705249	Håvard Gautneb	HG64-16	Medium grade graphite schist	0.18	1.12
137141	2016	Vardfjellet	607228	7705022	Håvard Gautneb	HG65-16	Medium grade graphite schist	0.09	4.56
137142	2016	Vardfjellet	607208	7705023	Håvard Gautneb	HG66-16	Medium grade graphite schist	0.38	5.43
137143	2016	Vardfjellet	607364	7705122	Håvard Gautneb	HG67-16	Medium grade graphite schist	0.20	3.99
137146	2016	Vardfjellet	608079	7704699	Janja Knezevic	JK1-020816	Medium grade graphite schist	0.24	6.42
137147	2016	Vardfjellet	607902	7705097	Janja Knezevic	JK2-020816	Low grade graphite schist	0.42	8.10
137148	2016	Vardfjellet	607834	7705137	Janja Knezevic	JK3-020816	Graphite schist in the contact zone of amphibolite/granit	1.32	6.92
137149	2016	Vardfjellet	607824	7705112	Janja Knezevic	JK4-020816	Folded graphite schist	0.09	14.07
137150	2016	Vardfjellet	607560	7705042	Janja Knezevic	JK4-208161	Amphibolite/graphite schist	0.19	6.69
137151	2016	Vardfjellet	607414	7705119	Janja Knezevic	JK-0808016	Folded graphite schist (end of big massive weathered outcrop)	0.49	4.32
90423	2014	Hesten	609632	7702107	Håvard Gautneb	HG23-14	Graphite schist	0.0447	3.08
90424	2014	Hesten	609632	7702107	Håvard Gautneb	HG24-14	Graphite schist	0.0299	4
90425	2014	Hesten	609632	7702107	Håvard Gautneb	HG25-14	Graphite schist	0.0646	3.09
90426	2014	Hesten	609430	7702309	Håvard Gautneb	HG26-14	Graphite schist	0.388	3.69
90427	2014	Hesten	609393	7702403	Håvard Gautneb	HG27-14	Graphite schist	0.01	5.38
90428	2014	Hesten	609396	7702427	Håvard Gautneb	HG28-14	Graphite schist	0.114	1.72
90429	2014	Hesten	609331	7702536	Håvard Gautneb	HG29-14	Graphite schist	0.0279	3.8
90430	2014	Hesten	609248	7702787	Håvard Gautneb	HG30-14	Graphite schist	0.0806	5.48
90431	2014	Hesten	609293	7702727	Håvard Gautneb	HG31a-14	Graphite schist	0.194	8.6
137111	2016	Hesten	609328	7702683	Håvard Gautneb	HG35-16	Medium graphite weathered graphite schist	0.20	10.37
137112	2016	Hesten	609368	7702499	Håvard Gautneb	HG36-16	Low grade graphite schist	0.74	3.50
137113	2016	Hesten	609245	7702815	Håvard Gautneb	HG37-16	Low grade graphite schist	0.10	7.92
137114	2016	Hesten	609243	7702817	Håvard Gautneb	HG38-16	Medium grade graphite schist	0.85	11.64
137115	2016	Hesten	609246	7702815	Håvard Gautneb	HG39-16	Medium grade and strongly weathered graphite schist	0.10	12.81
137116	2016	Hesten	609633	7702117	Håvard Gautneb	HG40-16	Medium grade and strongly weathered graphite schist	0.26	5.51
137117	2016	Hesten	609581	7702693	Håvard Gautneb	HG41-16	Medium grade and strongly weathered graphite schist	0.12	6.69

137118	2016	Hesten	609553	7702741	Håvard Gautneb	Hg42-16	Medium grade and strongly weathered graphite schist	0.08	5.76
137125	2016	Hesten	609056	7702936	Håvard Gautneb	HG49-16	Medium grade graphite schist	0.18	4.43
137126	2016	Hesten	609078	7702923	Håvard Gautneb	HG50-16	Medium grade graphite schist	0.16	5.73
137127	2016	Hesten	609089	7702916	Håvard Gautneb	HG51-16	Medium grade graphite schist	0.55	1.94
137128	2016	Hesten	609272	7702769	Håvard Gautneb	HG52-16	Medium grade graphite schist	0.33	6.14
137144	2016	Grunnvåg	617637	7702330	Håvard Gautneb	HG68-16	Rusty sulfide rich graphite schist	5.00	7.41
137145	2016	Grunnvåg	617697	7702362	Håvard Gautneb	HG69-16	Rusty sulfide rich graphite schist	0.85	8.46
137154	2016	Grunnvåg	617701	7702321	Janja Knezevic	JK-120816-2	Rusty sulfide rich graphite schist	4.58	14.85
137155	2016	Grunnvåg	617694	7702333	Janja Knezevic	JK-120816-3	Rusty sulfide rich graphite schist	12.50	6.72
137156	2016	Grunnvåg	617707	7702339	Janja Knezevic	JK120816-4	Rusty sulfide rich graphite schist/ outcrop along the stream	1.76	6.84

Appendix 2: Selected thin section images.

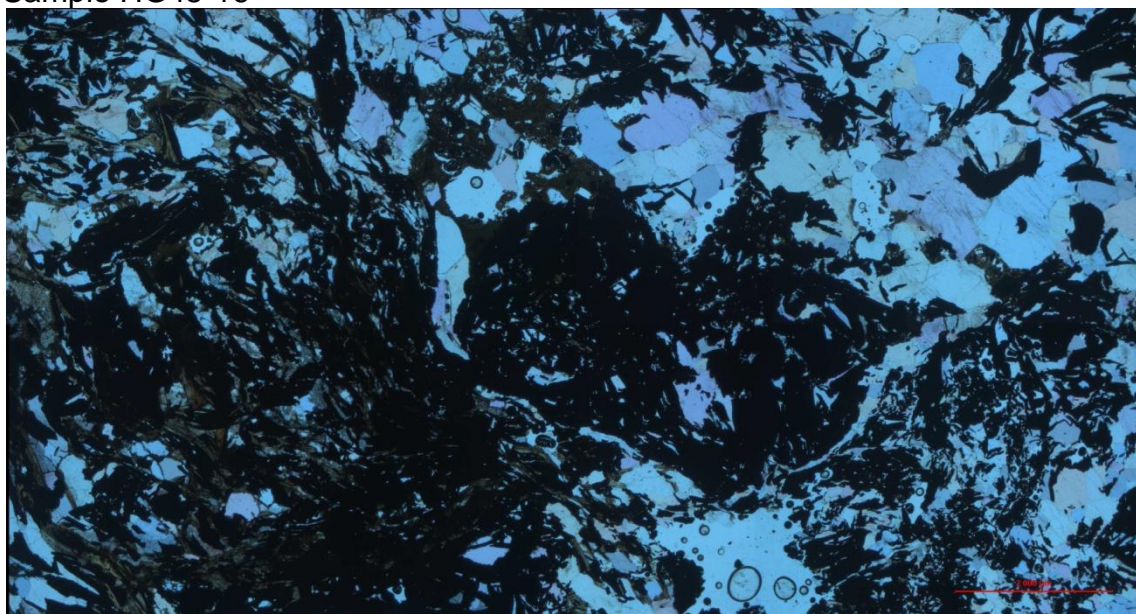
To illustrate the grain size distribution and internal mineralogical variation of the graphite bearing rocks, a selected set of thin section images is shown below.

Sample HG39-16



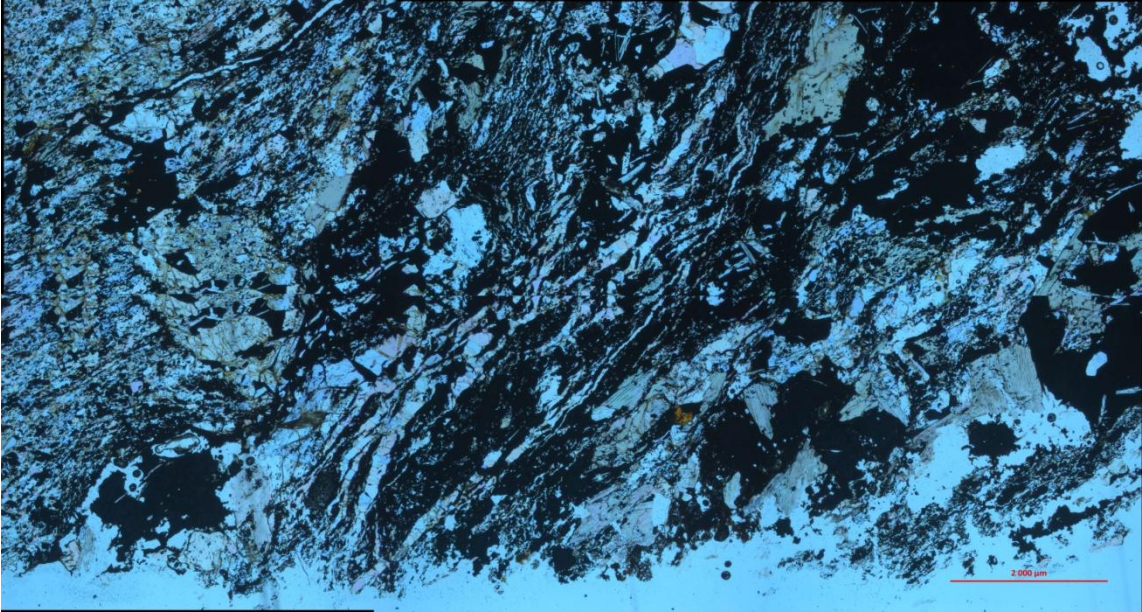
Graphite content 22.18 vol %

Sample HG45-16



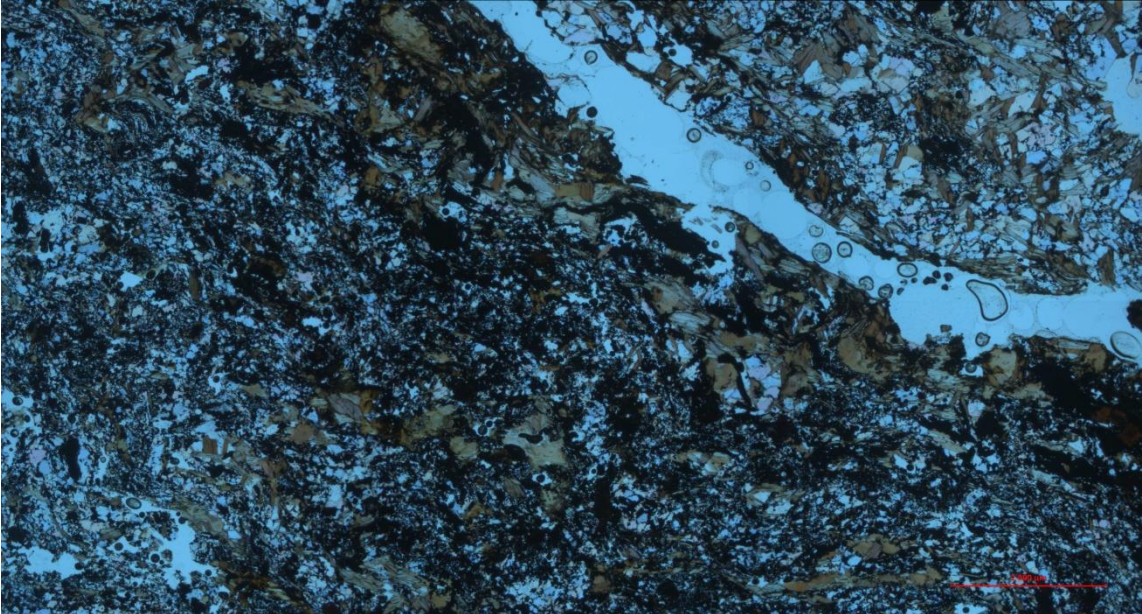
Graphite content 30.94 vol %

Sample JK120816-3



Graphite content 34.79 vol %

Sample JK4-020816-1

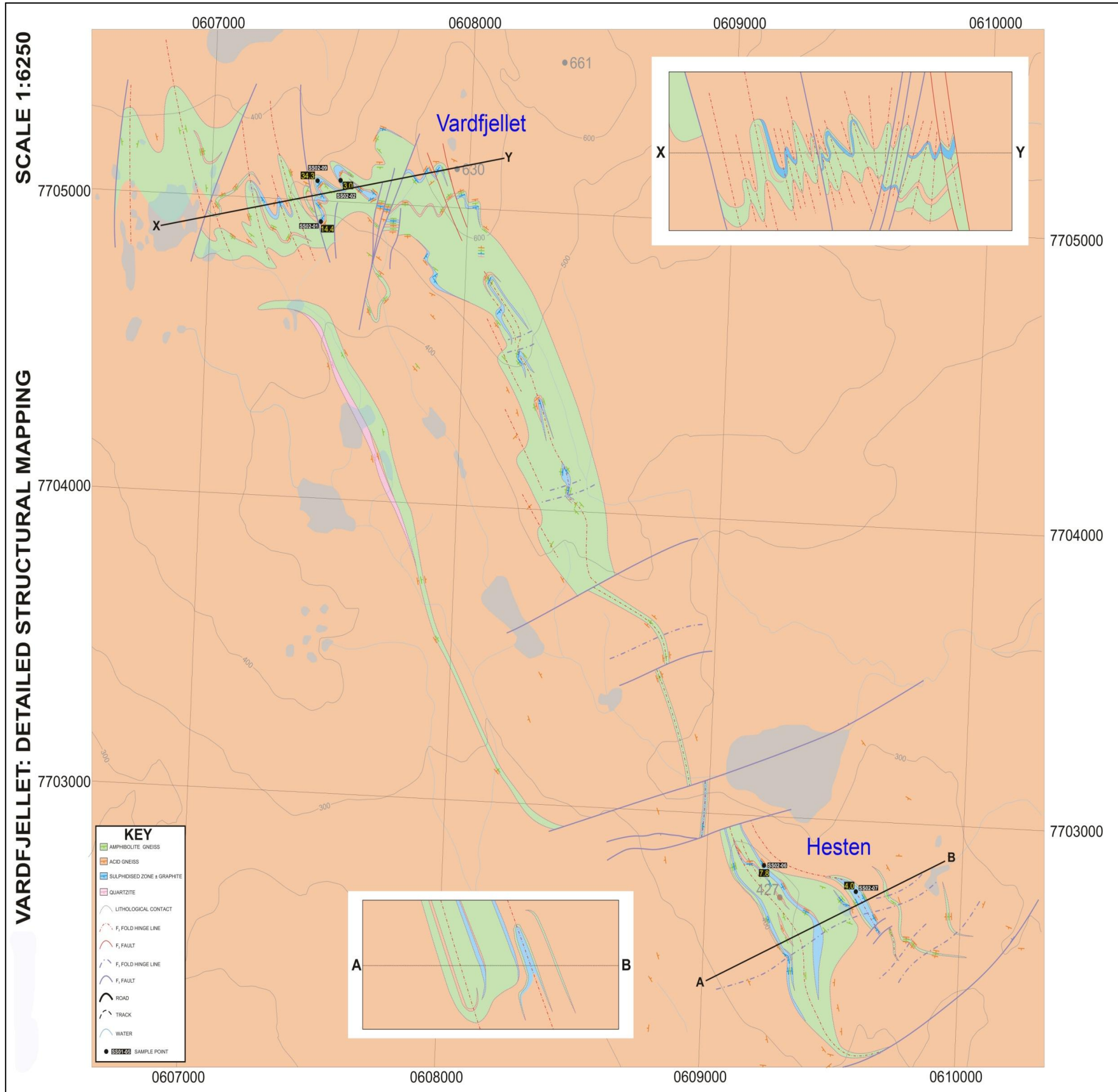


Graphite content 6.07 vol %

Sample no. JK20816-2



Graphite content 26.7 vol %



Appendix 3

Geological map over Vardfjellet and Hesten from Henderson & Kendrick (2003).
 The sulphidised zone contain in general less than 1% total sulphur.
 This mapping was done on paperbased topographic maps and individual graphite zones may be misplaced when compared with present day gps accuracy and our geophysical maps.



GEOLOGICAL
SURVEY OF
NORWAY

· NGU ·

Geological Survey of Norway
PO Box 6315, Sluppen
N-7491 Trondheim, Norway

Visitor address
Leiv Eirikssons vei 39
7040 Trondheim

Tel (+ 47) 73 90 40 00
E-mail ngu@ngu.no
Web www.ngu.no/en-gb/